



HAL
open science

Demise and recovery of Antillean shallow marine carbonate factories adjacent to active submarine volcanoes (Lutetian-Bartonian limestones, St. Bartholomew, French West Indies)

Vincent Caron, Julien Bailleul, Frank Chanier, Geoffroy Mahieux

► To cite this version:

Vincent Caron, Julien Bailleul, Frank Chanier, Geoffroy Mahieux. Demise and recovery of Antillean shallow marine carbonate factories adjacent to active submarine volcanoes (Lutetian-Bartonian limestones, St. Bartholomew, French West Indies). *Sedimentary Geology*, 2019, 387, pp.104-125. 10.1016/j.sedgeo.2019.04.011 . hal-03281151

HAL Id: hal-03281151

<https://hal.science/hal-03281151>

Submitted on 22 Oct 2021

HAL is a multi-disciplinary open access archive for the deposit and dissemination of scientific research documents, whether they are published or not. The documents may come from teaching and research institutions in France or abroad, or from public or private research centers.

L'archive ouverte pluridisciplinaire **HAL**, est destinée au dépôt et à la diffusion de documents scientifiques de niveau recherche, publiés ou non, émanant des établissements d'enseignement et de recherche français ou étrangers, des laboratoires publics ou privés.



Distributed under a Creative Commons Attribution - NonCommercial 4.0 International License

1 DEMISE AND RECOVERY OF ANTILLEAN SHALLOW MARINE CARBONATE
2 FACTORIES ADJACENT TO ACTIVE SUBMARINE VOLCANOES (LUTETIAN-
3 BARTONIAN LIMESTONES, ST. BARTHOLOMEW, FRENCH WEST INDIES)

4
5 Vincent CARON¹, Julien BAILLEUL², Frank CHANIER³, Geoffroy MAHIEUX¹

6
7 ¹EA 7511, Basins-Reservoirs-Resources (B2R), University of Picardie Jules Verne, Amiens,
8 France

9 ²EA 7511, Basins-Reservoirs-Resources (B2R), Institut UniLasalle, Beauvais, France

10 ³UMR 8187, Laboratoire d' Océanologie et de Géosciences (LOG), Lille, France

11 corresponding author (E-mail: vincent.caron@u-picardie.fr)

12
13 **ABSTRACT**

14 Among other parameters, volcanic activity adjacent to shallow marine environments influences
15 the development of ecosystems and their carbonate-producing communities. Volcaniclastic
16 sediment influx in particular has potential to cause rapid and drastic environmental changes
17 affecting biological systems in their composition and activity, and ultimately leading to changes
18 to and breaks in carbonate sedimentation. Such sedimentary breaks that form in response to
19 volcanic processes are rarely described in detail despite the common occurrence of carbonate
20 platforms adjacent to active volcanoes both in the recent and past geological record. The island of
21 St. Bartholomew (St. Barths), French West Indies, exposes sections of middle Eocene limestones
22 intercalated with thick volcaniclastic deposits and lavas. These carbonates provide an example
23 of a low-latitude tropical platform where non-framework building biota were important, if not

24 dominant, sediment contributors. The carbonate system records the repeated collapse and renewal
25 of carbonate production, as a result of episodic volcanoclastic material input. The discontinuous
26 nature of the carbonate sedimentation is reflected in contrasted depositional systems across
27 sedimentary surfaces and gradational contacts. The studied Eocene deposits provide a
28 sedimentary record of how volcanic events impacted warm-water carbonate factories, both in
29 their disturbance, demise and recovery.

30

31 **Keywords:** Eocene, Caribbean, carbonate ramp, skeletal carbonates, volcanoclastics

32

33 **1. Introduction**

34

35 Volcanism may be intuitively regarded as critically detrimental to shallow-water benthic
36 communities, and as such as one environmental parameter impacting the development of
37 carbonate platforms. Lava flows and large pyroclastic eruptions, either subaqueous or reaching
38 subtidal environments from emerged volcanoes, can undeniably result in mass mortality of
39 carbonate producers and therefore cause carbonate production to cease (Tomascik et al., 1996;
40 Vroom and Zgliczynski, 2011). However, recent studies have shown that volcanoclastic influx
41 may also allow carbonate-producing organisms with higher surviving capabilities to thrive, and
42 may promote a change of benthic communities, prolonging the existence of carbonate factories
43 (Wilson and Lokier, 2002; Lokier et al., 2009). These biota prove to be adapted to post-eruption
44 environmental conditions such as reduced luminosity and increased turbidity due to suspended
45 ash, change of substrate, change of nutrient levels and of water chemistry through alteration of
46 volcanic material (Reuter and Piller, 2011). It follows that volcanic events, even of short duration
47 and/or limited in the volume of material delivered to the marine realm, may be diversely

48 expressed in otherwise carbonate-dominated settings and ultimately in outcrops. Expected
49 physical, stratal and facies expressions of volcanoclastic influx include: (1) erosion of the seafloor
50 and of reefal buildups (Wilson, 2000); (2) reduction of or temporarily arrested carbonate
51 production; (3) deposition of volcanoclastic material; and (4) a change in the depositional systems
52 and in the biotic assemblages (Wilson and Lokier, 2002; Dorobek, 2008; Lokier et al., 2009;
53 Reuter et al., 2012).

54 Herein, we propose a depositional model for Eocene tropical carbonates that formed in a
55 volcanically active area, namely the Lesser Antilles Volcanic Arc, West Indies. Here, carbonate
56 and mixed carbonate-volcanoclastic units are intercalated between volcanoclastics and lava flows,
57 pointing to the repeated demise and foundering of carbonate factories, but also to the interplay
58 between volcanic activity and penecontemporaneous carbonate production. This study is the first
59 to document in detail the compositional characteristics of the Antillean carbonate successions on
60 St. Barths Island.

61

62 **2. Geological setting**

63

64 The Lesser Antilles arc is related to the westward-dipping subduction zone where the oceanic
65 crust of the American plate is underthrusting the Caribbean plate, hence causing important
66 volcanic and seismic activities (Fig. 1A).

67 North of the Island of La Martinique, the Lesser Antilles arc consists of two divergent volcanic
68 lines, namely the now extinct outer arc active from the early Eocene to middle Oligocene, and the
69 still active inner arc (Bouysse et al., 1990). Owing to this evolution and subsequent uplift, the
70 outer arc system became the locus of abundant carbonate production and accumulation during the
71 late Paleogene and Neogene. It evolved into extended carbonate platforms that correspond to the

72 so-called Limestone Caribbees, whereas to the west, intense volcanic activity led to the
73 construction of an archipelago of islands referred to as the Volcanic Caribbees (Bouysse et al.,
74 1990).

75 The Island of St. Barths lies on the northeastern sector of the Lesser Antilles outer arc and
76 belongs to the present-day platform. It consists predominantly of limestone beds intercalated
77 between volcanics (Fig. 1B). The latter includes hyaloclastite deposits generated by hydro-
78 explosions interbedded with andesitic and basaltic submarine lava-flows. Up to six limestone
79 sheets from 3 up to 40 m thick have been recognized and previously interpreted as peri-reefal
80 carbonates that were given a late middle Eocene (Lutetian and Bartonian) age on the basis of
81 microfaunal content (Westercamp and Andreieff, 1983a, 1983b; Gradstein et al., 2012). This
82 study concentrates on the limestone units and their under- and overlying contacts with volcanics.

83

84 **3. Methods**

85

86 *3.1. Field and laboratory analysis*

87

88 The bulk of information used in this study comes from field observation and description of 13
89 stratigraphic sections along the coasts of St. Barths and on two islets located southwest and
90 southeast off the main island, namely Pain de Sucre and Île Coco, respectively (Figs. 1C, 2).

91 Due to their common occurrence in the carbonate strata and locally in volcanoclastic units, and to
92 their relative abundance in some horizons associated with key sedimentary surfaces, echinoid
93 macrofossils were given special attention (Fig. 2). Field characteristics (diversity, abundance,
94 orientation and preservation) of spatangoid (*Schizaster* L. Agassiz, *Agassizia* L. Agassiz and
95 Desor, *Eupatagus* L. Agassiz, *Antillaster* Lambert) and oligopygoid (*Haimea* Michelin) echinoids

96 in particular, were determined prior to being collected where possible for taxonomic
97 identification. Echinoids include epibenthic dwellers and shallow to deep endobenthic burrowers
98 (Kier, 1984; Kanazawa, 1992; Donovan and Rowe, 2000). As such, echinoids are useful
99 indicators of paleoenvironmental conditions, including trophic resources, absence/presence of
100 seagrass beds, and substrate (Fig. 3). Characteristics of other dominant macrofossils, such as
101 corals and pinnids, were also evaluated qualitatively in the field (living position, mechanical
102 erosion, bioinfestation). In this study, the taxonomy of coralline algae uses at best generic names
103 only. Genus circumscription follows Rasser and Piller (1999) and Braga et al. (2009). Family to
104 subfamily names follow Harvey et al. (2003). Coralline algal growth-form terminology follows
105 Woelkerling et al. (1993). The taxonomy of larger foraminifera is restricted to Family level and at
106 best genus level except for those listed in Westercamp and Andreieff (1982, 1983).

107 The Eocene limestone units were analyzed petrographically using 110 thin-sections cut in
108 samples selectively collected below and above sharp, erosive, and burrowed contacts. The aim
109 was to provide estimates of the relative abundances of skeletal and non-skeletal constituents, and
110 to assess facies changes across sedimentary surfaces. Results were converted for the dominant
111 taxa at subfamily level and grain types into abundance indices of rare (one or two grains seen),
112 occasional (about 10%), common (conspicuous throughout, i.e., 20-30%), and abundant (the
113 grain category considered is the dominant skeletal component, i.e., $\geq 50\%$). The data obtained
114 were used to determine the composition of the skeletal associations only, and are not suitable for
115 statistical analysis. These qualitative data were complemented by textural information using the
116 criteria of Embry and Klovan (1971). In addition, a series of specific scales of taphonomic
117 features have been defined for various fossil types observed in thin section to help assess the
118 effects of early sea-floor processes, namely fragmentation, abrasion, bioerosion and encrustation

119 (Fig. 4).

120

121 *3.2. Skeletal associations*

122

123 Because pervasive bioturbation has obliterated, but in a few examples, primary wave- and
124 current-induced sedimentary structures, interpretation of the facies in terms of depositional
125 conditions was based on comparative ecology and sedimentology with ancient and modern
126 shallow marine environments (e.g., Hallock and Glenn, 1986; Hottinger, 1997; Bassi, 1998,
127 2005; Braga and Aguirre, 2001; Hallock, 2001; Hohenegger and Yordanova, 2001; Beavington-
128 Penney and Racey, 2004; Hallock et al., 2006; Hohenegger, 2009; Payros et al., 2010). Results of
129 the petrographic analysis highlight a diverse array of biotic constituents and skeletal associations,
130 which can satisfactorily be classified as chlorozoan, chloralgal and foramol (Lees and Buller,
131 1972; Lees, 1975; James, 1997), rhodalgal (Carannante et al., 1988), echinofor and foralgal
132 (Hayton et al., 1995). Although chloralgal and chlorozoan associations dominated by
133 zooxanthellate corals, calcareous green algae and non-skeletal carbonates (e.g., ooids, peloids and
134 oncoids) are robust indicators of relatively oligotrophic clear sea waters inside the tropical
135 climate belt, interpretation of the majority of skeletal associations in terms of temperature,
136 climate and paleoecology needs to integrate additional palaeoenvironmental information such as
137 nature of the substrate, siliciclastic fluxes and trophic resources (e.g., Hallock and Schlager,
138 1986; Hallock, 1985, 1987; Allmon, 1992; Brasier, 1995a, b; Pomar et al., 2004; Wilson and
139 Vecsei, 2005; Lokier et al., 2009; Reuter and Piller, 2011).

140

141 *3.4. Palaeoenvironments and paleodepths*

142

143 Although small isolated coral bioherms (patch-reefs s.l.) and coral carpets are present in some of
144 the limestone units, the absence of major reefal constructions (e.g., barrier coral-reef) and the
145 sedimentological characteristics of facies within the St. Barths limestones suggest that the general
146 depositional setting was a carbonate ramp (i.e., following the terminology of Burchette and
147 Wright, 1992) attached to and/or surrounding the flanks of active submarine volcanoes. The
148 subdivision of the carbonate ramp system into inner, middle and outer ramp depositional settings
149 follows the criteria proposed by Pomar (2001). The term inner ramp refers to depositional
150 environments between upper shoreface (i.e., the zone of breaking waves or lagoonal shorelines)
151 and Fair-Weather Wave Base (FWWB), middle ramp between FWWB and Storm-Wave Base
152 (SWB), and outer ramp below SWB (Burchette and Wright, 1992). The division of photic zones
153 with respect to water depths is based on the criteria of Pomar (2001). The low-light conditions
154 can be inferred from the absence or very rare co-occurrences of miliolids and calcareous green
155 algae (dasycladaleans), which typically are indicative of inner ramp environments when they are
156 the dominant biotic constituents (Geel, 2000; Zamagni et al., 2008).

157 The presence and abundance of taxa indicative of specific depth constraints known from modern
158 environments and interpreted from ancient deposits were only used to discriminate between
159 euphotic and oligophotic conditions (Pomar, 2001). Shallow-water biotic indicators include
160 zooxanthellate corals, pinnid bivalves, miliolids, conical agglutinated foraminifera and seagrass
161 dwellers such as small benthic rotaliids (Geel, 2000; Vecchio and Hottinger, 2007). The
162 estimation of paleodepth using trends in test flattening of larger benthic foraminifera, combined
163 with textural attributes of host sediments, namely siliciclastic content, grain size, and presence of
164 carbonate/argillaceous mud (Hohenegger et al., 2000; Beavington-Penney and Racey, 2004;
165 Cosovic et al., 2004; Hohenegger, 2009), suggests deposition in inner- to outer-ramp settings for
166 amphisteginids- and nummulitids-bearing deposits. Foralgal associations that include coralline

167 algae, such as dominant melobesioids (*Lithothamnion*, *Mesophyllum*) and subordinate
168 mastophoroids (*Lithoporella*) with rare sporolithales (*Sporolithon*) are generally associated with
169 middle-ramp to outer ramp settings (Nebelsick and Bassi, 2000; Braga and Aguirre, 2001; Pomar
170 et al., 2004). The abundance of flattened orthophragminids and planktic foraminifera points to
171 distal middle ramp to outer ramp settings (Bassi, 2005; Zamagni et al., 2008).

172 Changes in the depositional environments and in water depth thresholds for photodependent biota
173 are however to be expected in the immediate aftermath of volcanic eruptions due to clastic influx
174 and ash suspended in water (Wilson and Lokier, 2002; Lokier et al., 2009; Reuter and Piller,
175 2011; Reuter et al., 2012).

176

177 **4. Description of volcanoclastic deposits**

178

179 Volcanoclastic deposits represent the products of submarine eruptive episodes (Westercamp and
180 Andreieff, 1983a), and include a basal ensemble of arc tholeiites and an upper ensemble of calc-
181 alkaline series (Fig. 1B-C). Volcanoclastic deposits range in thickness from several tens of meters
182 to hundreds of meters. They are dominated by maar-type breccia (Vbr), coarse-grained
183 hyaloclastites (Hy), and medium- to fine-grained tuffs (Tu), in a proximal to distal distance
184 gradient from eruptive centers.

185 Coarse volcanoclastic breccia (Vbr) are massive to crudely bedded and contain heterometric
186 angular clasts ranging in size from gravel to boulder, in a coarse-grained tuffitic matrix. These
187 deposits are generally azoic, but may contain limestone clasts and coral heads reworked from
188 underlying limestone units (Fig. 5A-B).

189 Lithologies of coarse-grained hyaloclastites (Hy) and fine- to medium-grained tuffs (Tu) are
190 highly variable (see Westercamp and Andreieff, 1983b). The former can be subdivided into two

191 major groups, based on bedding structure and clast shape.

192 The first group (Hy1) consists of horizontal and low-angle tabular, fining-upward, dm-thick beds
193 having erosional bases. The basal contact is overlain by gravel- to cobble-sized (sub-)angular
194 volcanic clasts in a poorly-sorted sandy/gravelly matrix that grades into moderately sorted
195 volcanic sands (Fig. 5C).

196 The second group (Hy2) represents reworked hyaloclastites (Fig. 5D-E). The deposits
197 conformably overlie mixed carbonate-volcaniclastic limestones and exhibit alternating
198 poorly/moderately-sorted conglomeratic beds that contain sub-rounded coarse sand- to pebble-
199 sized volcanic clasts, and moderately-sorted coarse-grained volcaniclastic sandstones (Fig. 5E).
200 Bioclasts and macrofossils, including bivalves, gastropods, bryozoans, fragmented coral branches
201 and echinoids are common in the deposits.

202 Tuffs (Tu) include cm- and dm-thick tabular beds of silty to sandy, moderately- to well-sorted
203 deposits (Fig. 5F). Tuffs may be bioturbated and fossiliferous, with larger benthic foraminifera,
204 solitary corals, and spatangoids.

205

206 **5. Carbonate facies description**

207

208 A total of 15 facies have been distinguished that point to various environmental and
209 hydrodynamic conditions (Table 1). Features common to all facies are that none contain ooids or
210 evaporitic features.

211

212 *5.1. Mixed carbonate-volcaniclastic facies association (Mf1 to Mf5)*

213

214 The abundance of volcaniclastic, tuffitic, feldspar crystals and quartz grains characterize this

215 facies association. It can be subdivided into five major facies depending on the characteristics of
216 volcanoclastic components and on the biotic/non-skeletal carbonate particle content. Tuffitic
217 sediments, angular/subangular volcanoclastic fine sand to granule sized-debris and quartz fine-to
218 medium sand represent 20% to 50% of the sediment fraction.

219

220 5.1.1. Smaller foraminiferal – dasycladalean - coral photozoan mixed facies (Mf1 and Mf2)

221

222 Two biotic associations comprise this facies. Mf1 is a smaller foraminiferal-dasycladalean
223 association, and includes moderately- to well-cemented wackestones/floatstones, packstones and
224 more rarely grainstones. Mf2 includes dasycladalean-coral floatstones and coral boundstones.

225 Intense bioturbation produces a typical nodular aspect to facies Mf1 and Mf2 beds, though
226 massive bedding also occurs. Facies Mf1 and Mf2 strata may either overlie volcanoclastic units
227 across sharp and gradational contacts, or carbonate beds across sharp undulating and erosional
228 surfaces penetrated by *Thalassinoides* burrows.

229 In general, facies Mf1 is characterized by a low-diversity biota with a relative abundance of
230 smaller benthic foraminifera, and subordinate miliolids and dasycladalean algae (Fig. 6A).

231 Peloids may be common to abundant, and micritized grains are generally present. Agglutinated
232 conical foraminifera and laminar crusts of coralline red algae (*Lithoporella*) are occasional to
233 common (Fig. 6B). Other organisms, such as echinoids (*Eupatagus*, *Antillaster*), thin-walled
234 gastropods, bivalves, branching corals in living position and rare amphisteginids are also present.

235 Macrofossils and microfossils in micritic floatstones and wackestones/packstones show low to
236 moderate degrees of fragmentation and abrasion, low degrees of encrustation and moderate
237 degrees of bioerosion, except for corals which may be intensely bored. Grainstones typically
238 exhibit higher degrees of fragmentation and abrasion, lower encrustation, and similar bioinfection

239 of skeletal grains.

240 Facies Mf2 differs from Mf1 facies in being dominated by branching corals, which occur as spar-
241 filled moulds in a micritic matrix and constitute coral boundstones that locally build up small
242 patchreef frameworks. Thick-shelled gastropods, dasycladalean algae and miliolids may be
243 common. Large photosymbiont-bearing foraminifera are rare to common in places and include
244 amphisteginids and nummilitids. Agglutinated conical foraminifera and echinoid fragments are
245 present in small amounts. Other fossils include epifaunal spatangoids such as *Antillaster*.
246 Skeletons in facies Mf2 show low to moderate degrees of fragmentation and abrasion leaving
247 gastropods with their tubercles left intact for example. Corals are commonly partly micritized
248 and encrusted by cyanobacterial micritic laminae.

249

250 5.1.2. Echinoid – Red algal photozoan facies (Mf3)

251

252 Textural attributes of facies Mf3 are variable and range from wackestone to packstone/grainstone
253 (Fig. 6C). Massive bedding is typical, although nodular bedding also occurs pointing to intense
254 bioturbation that likely obliterated primary sedimentary structures.

255 Facies Mf3 is characterized by low-diversity biogenics with a relative abundance of echinoids
256 (plates and spine fragments) and fragments of rhodoliths, branches and laminar crusts. Larger
257 foraminifera are unusual, but when present consist predominantly of orthophragminids, and rare
258 nummulitids and amphisteginids. Micritic grains, such as peloids and cortoids, may be abundant.
259 Subordinate biogenics include bivalves and corals. Intraclasts are present and consist of skeletal
260 grains bearing rims of palisadic spar crystals with scalenohedral terminations and echinoid plates
261 with dirty spar syntaxial overgrowths. Facies Mf3 has moderate to high degrees of fragmentation
262 and abrasion, and relatively low to moderate degrees of bioerosion and encrustation.

263

264 *5.1.3. Mixed larger foraminiferal – mollusk photozoan facies (Mf4)*

265

266 The massive beds of facies Mf4 are sharp-based. Mollusks, larger ovate nummulitids,
267 amphisteginids and agglutinated conical foraminifera with particularly high amounts of coarse
268 sand to granule sized-volcaniclastics dominate these sediments. Volcaniclastic grains are sub-
269 angular and poorly- to moderately-sorted. Coral and coralline algal debris, and bryozoans are
270 occasional to common and typically show moderate to high degrees of fragmentation and
271 abrasion, little if any encrustation, and low bioerosional features. Echinoids are generally found
272 fragmented and include sand-dwellers *Eupatagus*, *Meoma* and *Haimea* (Fig. 3). Sedimentary
273 structures vary from planar bedding to sigmoidal and hummocky cross-stratifications. Facies
274 textures are volcaniclastic rudstones with a packstone and/or grainstone matrix.

275

276 *5.1.4. Mixed Bioclastic – peloidal facies (Mf5)*

277

278 Beds of facies Mf5 are either massive with a wavy basal contact or nodular grading from
279 underlying volcaniclastic deposits across a transitional interval of carbonate nodules in an
280 argillaceous matrix. Moderately to well-sorted silt and fine sand-sized bioclastic and tuffitic
281 material dominate this facies (Fig. 6D). The carbonate fraction consists predominantly of peloids
282 originating in micritized skeletal fragments, such as red algal debris, and of cortoids in a
283 packstone matrix. Subordinate components include fragmented benthic foraminifera, echinoid
284 plates and spines, and corals. Thin-shelled disarticulated bivalves may be present. Fragmentation
285 and abrasion are moderate, bioerosion is high and encrustation is rare.

286

287 5.2. *Dasycladalean - miliolid photozoan facies (DaMi)*

288
289 Beds of facies DaMi are massive. Wackestones and packstones are the dominant textures (Fig.
290 6E). Facies DaMi is similar to mixed facies Mf1 and Mf2, but is free of volcanoclastic content.
291 Smaller benthic foraminifera are common, and are associated with common to abundant
292 miliolids, dasycladalean algae and peloids. Accessory components include micritized grains
293 (cortoids), bivalves, agglutinated conical foraminifera (*Heterodictyoconus*), and occasional
294 amphisteginids. Laminar crusts of melobesioids are locally present. Rocks of facies DaMi contain
295 common branching corals and articulated bivalves in living position. Degrees of fragmentation
296 and abrasion are generally low, and bioerosion and encrustation are moderate to high.

297

298 5.3. *Larger benthic foraminiferal – coralline algal facies (LfRh, LfCa)*

299

300 This biotic association consists of packstones, rudstones and bindstones. Coralline algae are
301 represented by members of the subfamilies Mastophoroids (*Lithoporella*), Melobesioids
302 (*Mesophyllum*, *Lithothamnion*) and Sporolithalean (*Sporolithon*). Larger foraminifera are present
303 in all facies and are represented by amphisteginids, nummulitids (*Nummulites*), orthophragminids
304 such as *Discocyclusina*, *Pseudophragmina* and *Asterocyclusina*, and by the lepidocyclinid
305 *Polylepidina*. Accessory components comprise small benthic foraminifera (textulariids,
306 miliolids), encrusting foraminifera (acervulinids), fragments of bryozoans, bivalves, and corals.
307 Echinoid plates are locally common. Non-skeletal carbonates (peloids, oncoids, cortoids) are
308 generally present and may be abundant in places.

309

310 5.3.1. *Larger benthic foraminiferal – rhodolith photozoan facies (LfRh1 to LfRh3)*

311
312 These facies consist of coarse-grained packstones, sparitic rudstones/grainstones and rare
313 bindstones dominated by larger benthic foraminifera and coralline red algae. Decimeter-thick
314 beds have wavy bedding planes and are intensely bioturbated, resulting in a typical nodular
315 texture. Medium-scale (up to 1 m large and dm deep) trough cross-stratifications and low- to
316 high-angle foresets are locally present. The larger foraminiferal assemblage of facies LfRh1
317 consists of common amphisteginids, rare to occasional nummulitids, and lepidocyclinids. Facies
318 LfRh2 is a nummulitid-lepidocyclinid packstone-rudstone. Fragments of fruticose coralline thalli
319 and rhodoliths are also present in both facies and may be common to abundant within the
320 carbonate matrix. In addition, other biogenic components include occasional textulariids, rare
321 miliolids, occasional mollusks dominated by epifaunal bivalves, occasional coral fragments and
322 planktonic foraminifera. Peloids and cortoids range in abundance from rare to common. Coralline
323 bindstones are present locally in facies LfRh2 as intraclasts. The binding structure is composed of
324 laminar coralline thalli 0.5-1.0 mm thick and cyanobacterial laminae with a stromatolithic
325 texture. Mastophoroids (*Lithoporella*) and sporolithalean (*Sporolithon*) are present in facies
326 LfRh1, and rare to absent in facies LfRh2 and LfRh3. Facies LfRh3 is dominated by rhodoliths in
327 a bioclastic grainstone matrix composed of common echinoid plates and peloids, occasional
328 larger benthic foraminifera, mollusks, corals, and dasycladalean algae (Fig. 6F).
329 Rhodoliths in facies LfRh 1 and LfRh2 are variable in size with a mean diameter from 1 to 10
330 cm, and are typically dispersed within a coarse-grained grainstone matrix. Coalescence of two
331 rhodoliths has been observed. Rhodoliths in facies LfRh3 are more homogeneous in size ranging
332 from 1-5 cm. The most common rhodolith morphology is sub-spheroidal with a dense inner
333 laminar arrangement of coralline thalli. Epifaunal macrofossils include irregular echinoids
334 *Haimea* and *Antillaster*, and large thick-shelled oysters, which may locally be abundant in facies

335 LfRh1.

336 There is no significant difference between facies LfRh1, LfRh2 and LfRh3 in their degree of
337 taphonomic alteration. Each facies consists of a mixture of poorly to highly altered skeletal
338 material with respect to fragmentation, abrasion and bioerosion. Encrusters include red algae,
339 serpulids, foraminifera, and cyanobacteria.

340

341 *5.3.2. Larger benthic foraminiferal – coralline algal photozoan facies (LfCa1 and LfCa2)*

342

343 Facies LfCa1 and LfCa2 consist of massive- to nodular-bedded larger foraminiferal-red algal
344 packstones and grainstones. Basal contacts are either gradational or sharp. Underlying strata are
345 mixed carbonate-volcaniclastic and carbonate units. The main components are coralline algal
346 branches, less than 1 cm-sized rhodoliths, and their debris, and larger benthic foraminifera.

347 Among the latter, amphisteginids and subordinate nummulitids dominate facies LfCa1 (Fig. 6G),
348 whereas nummulitids associated with orthophragminids are abundant in facies LfCa2 (Fig. 6H).

349 Other dominant components include echinoid plates and spines, smaller benthic foraminifera
350 (rotaliids and occasional textulariids), and peloids and micritized skeletons. Subspheroid

351 rhodoliths (up to 3 cm in diameter) may also be present. Coralline branches and debris consist
352 mostly of melobesioids and occasional mastophoroids (*Lithoporella*).

353 The foraminiferal assemblage is dominated by *Amphistegina* and *Nummulites* in LfCa1, and
354 *Nummulites*, *Discocyclusina* and *Pseudophragmina* in LfCa2.

355 Skeletal material in facies LfCa1 has lower degrees of alteration than its counterpart in facies
356 LfCa2. In the latter, coralline thalli and larger foraminifera exhibit a wide range of alteration from
357 low to high for fragmentation, abrasion, bioerosion and encrustation, pointing to the mixing of
358 fresh and older skeletons, i.e., exposed for longer periods of time to destructive processes.

359

360 5.4. *Echinoid facies associations (EcF1 and EcF2)*

361

362 Facies EcF1 are well-cemented packstones and grainstones containing abundant echinoid
363 fragments, common peloids and subordinate larger benthic foraminifera (Fig. 6I). Beds of facies
364 EcF1 are massive to nodular with sharp basal contacts. Facies EcF2 are semi-lithified packstones
365 and wackestones rich in small benthic foraminifera (rotaliids), and comprise a complex
366 assemblage of echinoid macrofossils. Decimeter-thick beds of facies EcF2 generally overlie
367 wavy surfaces pervasively bioturbated by *Thalassinoides*.

368

369 5.4.1. *Echinoid – non-skeletal carbonate photozoan facies (EcF1)*

370

371 Irregular echinoids, including spatangoids (*Haimea*) and cassiduloids (*Echinolampas*) are
372 common in these rocks. Branching zooxanthellate corals in growth position are ubiquitous at
373 some localities. Gastropods and disarticulated bivalves are present. The fine- to medium-sand
374 sized biogenic particles comprise common to abundant echinoid plates (Fig. 6I), occasional larger
375 benthic foraminifera, particularly amphisteginids and nummulitids, molluskan fragments,
376 geniculate and non-geniculate coralline debris, and less common miliolids, small agglutinated
377 foraminifera, coral debris, and bryozoans. Peloids are common to abundant. Frequent presence of
378 micritized skeletons suggests that the majority of peloids may be small micritized grains.

379 Degrees of fragmentation and abrasion are moderate to high, and common micritization indicates
380 that bioinfestation is pervasive. Encrustation of coral fragments and mollusks is low to moderate,
381 and involves cyanobacteria, red algae and foraminifera.

382

383 5.4.2. *Echinoid – smaller benthic foraminiferan photozoan facies (EcF2)*

384

385 The co-occurrence of spatangoids, cassiduloids, and oligopygoids with different living habitats
386 and substrate dependencies is frequent in facies EcF2 deposits. The co-occurrence of *Haimea*,
387 *Schizaster*, *Agassizia*, *Eupatagus*, and *Echinolampas* provides an example of such complex
388 diverse echinoid assemblages (Fig. 3) that point to contrasted depositional conditions over time.
389 Results show that about 30% echinoids are in living position, a majority of which (80%) being
390 represented by shallow (*Agassizia*) and deep (*Schizaster*) infaunal dwellers. Other macrofossils
391 include large thick-shelled gastropods and pinnid bivalves dispersed in the deposits. Foraminifera
392 comprise the porcelaneous and hyaline smaller benthic majority. Larger forms are occasional.
393 Coralline fragments are rare and tend to be dominated by geniculate forms. Small agglutinated
394 foraminifera, mollusks, miliolids, and calcispheres are occasional. Peloids may be abundant,
395 whereas cortoids and oncoids are unusual. Volcaniclastic content is low.

396 The skeletal fraction has moderate to high degrees of fragmentation and abrasion, low to
397 moderate degrees of bioerosion and encrustation. However, echinoid plates are typically less
398 affected by destructive processes than other skeletons.

399

400 5.5. *Coral photozoan facies (CoP1 and CoP2)*

401

402 Two facies that reflect different biohermal geometries, hydrodynamic conditions and coral shapes
403 are present. Members of the genera *Astrocoenia*, *Hydnophora*, and *Cladocora* have been
404 identified. Small bioherms with lenticular geometry, a few meters large and up to 2-4 m high, and
405 coral carpets characterize facies CoP1. Branching and platy corals in growth position constitute
406 the coral framework. Corals are enclosed in a peloidal-micritic matrix. Other components include

407 encrusting coralline algae, gastropods and small benthic foraminifera. Meter-sized lenticular
408 bioherms exhibit several growth-phases, each one being laterally correlated to tabular beds of
409 facies Mf2, EcF2, and DaMi (Fig. 7A), a geometry that reflects a strong interaction between
410 biohermal building and ambient sedimentation (Gaillard, 1983). Massive coral framework and
411 biohermal rudstones compose facies CoP2. Individual biohermal structures are up to 6-8 m-high.
412 Massive dendroid corals in living position dominate in the upper half part of the constructional
413 bodies (Fig. 7B). Pebble to cobble-sized reef debris constitute lateral correlatives of the coral
414 build-ups and are deposited as structureless up to 1 m-thick beds intercalated between tabular and
415 nodular beds of facies EcF1 and LfCa1. The base of the coral build-ups appear sharp and possibly
416 erosional (Fig. 7B), though not confirmed by field observation, a discrepancy that may originate
417 in differential compaction and diagenesis (Rusciadelli and Di Simone, 2007; Berra and
418 Carminati, 2012).

419

420 **6. Carbonate facies interpretation**

421

422 The virtual absence of silty micrite-rich planktonic foraminifera-dominated facies indicates that
423 St. Barths Eocene carbonates and mixed carbonate-volcaniclastic sediments were principally
424 deposited in inner to middle ramp settings (Nebelsick et al., 2005). In addition, the rare to
425 occasional occurrence of symbiont-bearing larger benthic foraminifera with flattened shapes
426 (orthophragminids, lepidocyclinids), a morphological adaptation to maximize light collection in
427 otherwise oligophotic conditions below wave influence (Hallock and Glenn, 1986; Beavington-
428 Penney and Racey, 2004; Hohenegger, 2009), and of light-independent biota-dominated facies
429 confirm that the studied deposits are representatives of inner ramp and proximal to possibly distal
430 middle ramp facies belts. Figure 8 proposes a reconstruction of the depositional environments

431 envisaged for the St. Barths carbonate facies. We must emphasize that different microfacies
432 associated with identical parts of the carbonate ramp may not have all developed
433 contemporaneously, even though a mosaic of subenvironments, each being characterized by
434 specific ecological attributes in relation to subtle or major changes in substrate, nutrient levels,
435 water depth, salinity and/or other parameters, should be expected in settings influenced by
436 volcanism, subsequent influxes of volcanoclastics and resulting environmental stresses.

437

438 *6.1. Inner ramp: shallow back barrier setting and patch reefs*

439

440 Biogenic assemblages dominated by euphotic taxa, sedimentary structures comprising thin and
441 planar beds, and micritic textures of facies Mf1, Mf2, Mf5, DaMi, CoP1 and EcF2 (Table 1) are
442 interpreted to signal shallow-water inner ramp environments. The abundance of smaller benthic
443 foraminifera, including textulariids, the common occurrence of dasycladid algae, miliolids,
444 agglutinated conical foraminifera, and the rarity of hyaline larger foraminifera in facies Mf1
445 suggest light-level conditions of the upper euphotic zone (Murray, 1991; Geel, 2000; Zamagni et
446 al., 2008). The presence of delicate laminar crusts of mastophoroid coralline algae, which appear
447 detached from their substrate and commonly exhibit hook and ring shapes (Fig. 6E), together
448 with common calcareous green algae fragments and smaller benthic foraminifera hint for the
449 existence of seagrass beds in the depositional environment (Sola et al., 2013).

450 The local abundance of coral colonies constructing isolated bioherms, the presence of larger
451 foraminifera and the occasional occurrence of smaller benthics suggest normal marine salinities
452 such as in facies Mf2 and DaMi.

453 Fossils of these facies and their taphonomic attributes, together with wackestone and packstone
454 textures and sedimentary structures, indicate low-energy hydrodynamic conditions in shallow-

455 water. The abundance of miliolids, together with spatangoids *Schizaster* and *Brissoides* (Fig. 3)
456 points to soft fine-sand and muddy substrates. The abundance of volcanoclastics in mixed facies
457 likely resulted in coarser substrates favorable to epifaunal and shallow endofaunal dwellers, such
458 as *Antillaster* and *Eupatagus* (Kanazawa, 1992; Donovan and Rowe, 2000). Although the final
459 depositional setting for facies EcF2 sediments is interpreted to be a shallow protected
460 environment (i.e., occurrence of spatangoid dwellers and mud-dominated deposits), the diverse
461 echinoid assemblage pointing to varied palaeoecological modes (i.e., from sand to muddy
462 substrates; Fig. 3) associated with high fragmentation and abrasion indices of the bioclastic
463 fraction implies a complex depositional history from high/moderate- to low-energy
464 hydrodynamic conditions.

465 Abundance of volcanoclastic elements in carbonate strata overlying volcanoclastic units across
466 erosive surfaces (see discussion below) suggests reworking of underlying beds through wave
467 action.

468

469 *6.2. Open inner ramp to middle ramp: wave-dominated settings*

470

471 Open inner ramp and transitional environments to middle ramp settings are dominated by wave
472 action. The influence of currents and high-energy waves can be deduced from the lack of easily
473 winnowed silts and micrite, relatively coarse grain sizes, moderate to high degrees of
474 fragmentation and abrasion of skeletons and lithoclasts, and cross-stratifications. In addition,
475 robust coral morphologies and overall thick-walled skeletons more resistant to wave-induced
476 transportation and to waterborne projectiles constitute useful indicators of strong hydrodynamic
477 conditions (Hughes, 1987).

478 Representative of inner ramp to middle ramp facies belts are facies LfRh1, LfCa1, Mf4, EcF1

479 and CoP2 (Table 1). With the exception of chlorozoan facies (CoP2), most facies are
480 characterized by diverse faunal assemblages with varied degrees of alteration.

481 The dominance of biotic assemblages with robust larger foraminifera (*Amphistegina*,
482 *Nummulites*, and subordinate *Discocyclusina*), coralline algal branches, subspheroid rhodoliths,
483 together with the presence of zooxanthellate corals and smaller benthic foraminifera, miliolids
484 and dasycladal algae, indicate deposition within the euphotic zone (Pomar, 2001; Nebelsick et al.,
485 2005; Afzar et al., 2011). The common occurrence of larger foraminifera argues against high
486 nutrient levels, since these foraminifera thrive in mesotrophic to principally oligotrophic waters
487 (Hottinger, 1997; Langer and Hottinger, 2000; Halfar et al., 2004).

488 Constituents of these coarse-grained facies (packstones, grainstones and sparitic rudstones)
489 possess moderate to high degrees of fragmentation and abrasion consistent with relatively high-
490 energy deposition above FWWB (Burchette and Wright, 1992). Particularly, the common
491 occurrence of broken, poorly-preserved and abraded larger foraminifera not only provides
492 evidence of high-energy conditions, but also may indicate repetitive burial and exhumation due to
493 frequent physical reworking (Beavington-Penney, 2004).

494 Low- to high-angle cross-stratifications may represent internal structures of subaqueous skeletal
495 dunes that developed through the reworking of bottom sediments including inner ramp protected
496 smaller foraminiferal – miliolid – dasycladalean sediments and deeper, more open, hyaline
497 foraminiferal – coralline algal deposits. Sigmoidal and hummocky cross-stratifications record
498 wave-dominated hydrodynamic conditions (Dumas and Arnott, 2006; Tinterri, 2011).

499 Similar inner to middle ramp packstones and grainstones dominated by larger foraminifera and
500 coralline algae with comparable sedimentary attributes and occasional coral occurrences have
501 been documented in south-east Asia from Eocene to middle Miocene limestones (Adams, 1965;
502 Wilson et al., 2000; Wilson, 2002; Wilson and Lokier, 2002), in the Indus Basin from Paleogene

503 limestones (Afzal et al., 2011), and in other Paleogene western Tethyan deposits (e.g., Loucks et
504 al., 1998) for example. In the Caribbean realm, the middle Eocene Swanswick Formation of the
505 White Limestone Group of Jamaica contains a diverse larger foraminiferal-algal assemblage with
506 common echinoderm and molluskan fragments that Mitchell (2004, 2013) similarly interpreted as
507 open marine high-energy platform deposits.

508

509 *6.3. Distal middle ramp facies belt: episodic wave influence*

510

511 Middle ramp deposits are represented by foralgal and rhodalgal associations of facies LfRh2,
512 LfRh3, Mf3, and LfCa2 (Table 1). The dominance of wackestones and packstones, and
513 subordinate grainstones are compatible with low-energy conditions allowing settlement of fine
514 particles, alternating with episodes of high-energy wave events (Burchette and Wright, 1992;
515 Nebelsick et al., 2005; Afzal et al., 2011). Abraded rhodoliths and the common occurrence of
516 algal debris, and other bioclastic, material are supportive of current or wave reworking. Similar
517 features have been recognized in open marine platforms influenced by sporadic storms (Lund et
518 al., 2000), and fossil examples have been described from Cenozoic successions (Braga and
519 Martin, 1988; Bassi, 2005; Barattolo et al., 2007; Payros et al., 2010). The regime of waves and
520 currents is an important factor that determines the shape and internal structure of rhodoliths (e.g.,
521 Freiwald, 1995; Marrack, 1999). As such, the coalescence of rhodoliths (Fig. 6F) suggests times
522 of relative hydrodynamic quiescence between episodes of turbulence preventing burial by fine
523 sediments. The coralline algal assemblages are dominated by melobesioids with accessory
524 mastophoroids and sporolithaceans. Compared to facies interpreted as inner ramp deposits, there
525 is a taxonomic variation corresponding to a relative decrease in mastophoroids (*Lithoporella*)
526 and sporolithaceans (*Sporolithon*), and an increase in melobesioids (*Lithothamnion*). Such

527 taxonomic changes in coralline assemblages showing a depth gradient have fossil analogues
528 (Rasser, 2000; Braga and Aguirre, 2001; Aguirre et al., 2017) and have been documented in
529 modern settings (Iryu et al., 1995). A distal middle ramp setting is compatible with the
530 foraminiferal assemblage dominated by nummulitids and orthophragminids, with subordinate
531 lepidocyclinids, rare amphisteginids and occasional planktonic foraminifera (Nebelsick et al.,
532 2005). In addition, the occasional occurrence of flattened test morphologies but also of light-
533 dependent organisms, and the abundance of coralline algae suggest depositional conditions below
534 FWWB and above SWB (Hottinger, 1997; Hohenegger et al., 2000; Bassi, 2005; Hohenegger,
535 2009).

536

537 **7. Discussion**

538

539 Specific to carbonate systems is that any significant change of either one of the parameters, (e.g.,
540 trophic resources, depth of light penetration, turbidity, nature of substrate, etc.) influencing
541 carbonate factories will result in either temporary or prolonged halts in carbonate production and
542 accumulation in different sectors of the shelf (Wilson, 2000; Wilson and Lokier, 2002; Wilson
543 and Vecsei, 2005; Lokier et al., 2009; Reuter et al., 2012). St. Barths limestones record the
544 repeated collapse and renewal of carbonate production, as a result of episodic volcanoclastic
545 material input (see below; Figs. 9, 10).

546

547 *7.1. Demise of carbonate factories*

548

549 Submersion and drowning caused by relative sea-level changes, environmental deterioration and
550 burial by clastics are major controls on the demise of tropical carbonate platforms (Schlager,

551 1989). Termination of St. Barths carbonate factories relates to volcanoclastic input with
552 accumulation rates exceeding rates of skeletal carbonate production and reef building until burial.
553 Erosional and sharp sedimentary surfaces between carbonate deposits below and volcanoclastic
554 above are the dominant stratigraphic expressions identified in the studied successions for the
555 demise of carbonate factories (Figs. 11A-D, 12).

556 Erosional surfaces are overlain by polymictic matrix-supported breccias (Facies Vbr), and
557 represent syneruptive surfaces generated by the discharge of coarse volcanic material in the
558 carbonate realm (Figs. 2B, 5B, 10A, 11A-B) (Trofimovs et al., 2006). Sharp surfaces represent
559 sedimentation events (Reading, 1996) and coincide with the abrupt transition from carbonate to
560 volcanoclastic sedimentation, dominated by hyaloclastites of facies Hy1, with minor if any
561 evidence of erosion and bioturbation (Figs. 11C, 12A). Such sharp non-erosional surfaces have
562 been interpreted to reflect insufficient skeletal production of carbonate systems compared to the
563 rates of clastic accumulation (Schlager, 1989; Wilson, 2002; Lokier et al., 2009). Suffocation of
564 carbonate factories by volcanoclastics was likely facilitated by the rarity of significant coral reef
565 buildups and the predominance of slow carbonate producing biota (Reuter, 2011), such as
566 foraminifera and coralline red algae, in the St. Barths limestones.

567 Gradational contacts also occur and represent progressive burial of carbonate systems by
568 volcanoclastics of facies Hy1 and Hy2 (Figs. 2C, 11D, 12B). They indicate that prolongation of
569 carbonate production during volcanoclastic input was possible provided a change of benthic
570 communities from soft muddy to gravelly-shelly substrate dwellers having the capability to
571 escape burial such as irregular echinoids (from LfCa1 to facies Mf4; Fig. 11D). Low- to high-
572 angle cross-stratifications in the overlying volcanoclastic deposits (Figs. 11D, 12B) suggest that
573 volcanoclasts were transferred, considering the proximity of volcanic centers (Fig. 1), downslope
574 via dunes, sand waves or in avalanche flows (Caron et al., 2004; Dorobek, 2008; Puga-Bernabéu,

575 2010).

576

577 *7.2. Temporary halts in carbonate production and deposition*

578

579 Within the studied Eocene carbonate successions burrowed surfaces, interpreted as omission
580 surfaces, are of particular interest since some of them are associated with tuffitic layers (Figs. 9,
581 10B, 11H-J, 12).

582 Omission surfaces are emphasized by a complex network of *Thalassinoides* burrows reaching
583 their maximum density beneath the surface and decreasing downwards (Figs. 2D, 11I, 12C-H).

584 Most published works relate omission surfaces to stratigraphic condensation during periods of
585 slowed/non-deposition (e.g., Clari et al., 1995; Hillgärtner, 1998; Christ et al., 2012). Sediments
586 by-pass, drained siliciclastic sources, wave- and/or current-induced sediment transfer and
587 submarine erosion are major factors considered to promote non-deposition on the sea floor.

588 Previous authors have tied the formation of omission surfaces to specific portions of relative sea-
589 level cycles where the position of the sea floor relative to the wave base is considered a key
590 parameter to the onset of omission (Lukasik and James, 2003; Christ et al., 2012). However, an

591 alternative explanation for the genesis of omission surface can be proposed based on the

592 assumption that starved sedimentation may also result from the interruption of *in situ* carbonate
593 production below and above fair-weather wave base. Although some organisms (e.g., Bivalves

594 and Echinoids) have the ability to extricate themselves if buried beneath sediments and others to
595 remove fine particles from their surface (Hinchey et al., 2006; Lokier et al., 2009; Knoll et al.,

596 2017), episodic volcanic eruptions delivering high amounts of volcanoclastic material including
597 ash (Fig. 10B) will result in rapid physical burial and consequent mass-mortality of benthic

598 communities (Heikoop et al., 1996; Tomascik et al., 1997; Alve, 1999; Reuter and Piller, 2011).

599 The formation of omission surfaces depends on the duration of sediment starvation, and therefore
600 here the time span between volcanic events and the recovery of carbonate factories. Where
601 volcanoclastics were deposited above wave base, resuspension of their finer portion is likely to
602 result in higher turbidity and in reduced light levels, thereby delaying the reestablishment of
603 photodependent organisms (Hallock and Glenn, 1986). In addition, the potential increase of
604 nutrient input through chemical alteration of volcanic particles may cause eutrophication at the
605 sea floor and prevent colonization by oligotrophic and mesotrophic communities (Hallock and
606 Schlager, 1986; Allmon, 1992; Brasier, 1995a; Hallock, 2001; Reuter and Piller, 2011). The time
607 frame for either full recovery of the benthic communities that existed prior to the volcanic event
608 or the renewal of carbonate systems via a switch to different biotic assemblages is difficult to
609 estimate from the geological record but examples in the literature point to reestablishment over
610 decades and centuries (Heikoop et al., 1996; Tomascik et al., 1996; Pandolfi et al., 2006; Reuter
611 et al., 2011; Vroom and Zgliczynski, 2011). This time frame is compatible with the development
612 of a dense burrowing network and of omission (Dashtgard et al., 2008).

613

614 *7.3. Recovery and renewal of carbonate factories (Fig. 13)*

615

616 Besides light conditions and nutrient levels, periods of volcanic quiescence and reduced
617 availability of volcanoclastic material were likely the principal promoting conditions for the
618 renewal of carbonate production. In the studied successions, mixed facies (Mf1-Mf3) followed by
619 open marine foralgal (larger foraminifera-coraline algal facies; LfCa) and rhodalgal facies
620 (LfRh) occur above erosional surfaces cut in sandy to gravely volcanoclastic substrates (Figs.
621 11F, 13C). Protected lagoonal foralgal facies (dasycladalean-miliolid facies; DaMi) are found
622 above omission surfaces capping silty-sandy substrates and above marly concretionary horizons

623 grading from sand-sized volcanoclastics (Figs. 2C, 11E, 13E-F). Echinofor facies (echinoids-
624 larger foraminifera; EcF) capped by coral carpets locally represent the initial carbonate
625 development above gradational contacts. A review of foundering photozoan carbonate facies
626 described in the literature shows similar colonizing biota on siliciclastic substrates (e.g., Hendry
627 et al., 1999; Wilson, 2002; Burton, 2004; Lokier et al., 2009; Reuter and Piller, 2011; Reuter et
628 al., 2012). Rhodolith-bearing units similar to those reported here (Fig. 11F), and located above
629 erosional unconformities cut in rocky and clastic substrates, have been interpreted as
630 transgressive deposits sitting on surfaces of marine erosion (e.g., Nalin et al., 2007). Gradational
631 contacts have been inferred to record a progressive decrease of siliciclastic input and subsequent
632 colonization by carbonate producers reflected in transitional mixed facies (e.g., Hendry et al.,
633 1999; Burton, 2004; Lokier et al., 2009).

634 Characteristics of the renewal of carbonate production described here suggest that they may result
635 from a combination of factors promoting the reduction of volcanoclastic influx (e.g., changes in
636 sediment transport direction and volcanic quiescence) and relative sea-level changes. Marly
637 horizons at the volcanoclastic-carbonate interface, erosional and sharp-cut surfaces (Fig. 13A-B)
638 are compatible with marine flooding. However, deepening-upward trends in facies above these
639 surfaces have not been observed. This discrepancy might be explained by a slow rise of relative
640 sea-level allowing aggradation without significant change of carbonate-producing biota.

641

642 **8. Conclusions**

643

644 The main results of the present study and their broader implications for the analysis of carbonate
645 successions in volcanically-active settings may be summarized as follows.

646 1 The middle Eocene limestones of St. Bartholomew Island contain marine depositional facies

647 characteristic of inner to distal middle ramp settings affected by episodic volcanic eruptions. The
648 variety of carbonate-producing biota (i.e., chlorozoan, chloralgal, foralgal), in terms of their
649 dependence to light intensity and tolerance to nutrient levels, suggests that carbonate production
650 occurred mostly in euphotic conditions across an unrimmed platform with isolated coral
651 bioherms and shoals. Other biogenic contributors (i.e., rhodalgal, echinofor) are consistent with
652 oligophotic conditions related to resuspended fine material after storms or fine volcanoclastics
653 input following eruption that diminished water transparency. The St. Barths Eocene carbonates
654 provide an example of low-latitude tropical platform where non-framework building biota were
655 important, if not dominant, sediment contributors, compared to other Eocene carbonate deposits.

656 2 This study shows that the effects of volcanism on carbonate factories range from burial and
657 prolonged termination of carbonate factories, to temporarily arrested or slowed carbonate
658 production. When volcanoclastic inputs ceased, carbonate systems reestablished. Foundering
659 biotic communities include euphotic chlorozoan facies, oligophotic foralgal, rhodalgal and
660 echinofor facies mixed in various proportions with volcanoclastics.

661 3 The discontinuous nature of the carbonate sedimentation in relation to volcanoclastic influx is
662 reflected in: (a) erosional and sharp sedimentary surfaces that mark pronounced facies changes;
663 and, (b) gradational contacts.

664 Some sedimentary surfaces and contacts located at volcanoclastic-carbonate boundaries record the
665 renewal of carbonate production above volcanoclastic deposits, while others record either the
666 temporary halt of carbonate production or the demise of carbonate platforms buried beneath thick
667 volcanoclastics.

668 The demise of carbonate factories and their prolonged shut-down in the vicinity of active
669 volcanoes originated in the propagation of syneruptive pyroclastic flows or in the
670 progradation/migration of wave-reworked volcanoclastic material, eroding and burying carbonate

671 deposits. Temporary shut-down of *in situ* carbonate production also occurred and was likely a
672 result of environmental stresses caused by fine volcanoclastics, including burial, lowered light
673 levels and eutrophication.

674 The recovery of carbonate factories resulted from an interruption of volcanoclastic influx at the
675 onset of volcanic quiescence promoting the reduction of volcanoclastic influx at the locus of
676 renewed carbonate production.

677 Future investigations should concentrate, in a broader regional context, on the characterization of
678 key sedimentary surfaces and discontinuities in mixed volcanoclastic-carbonate successions of the
679 Volcanic Arc Antillean area. Correctly interpreting the origin and significance of discontinuities
680 in carbonates deposited adjacent to active volcanoes is important to avoid misinterpretation of
681 other key surfaces in a cyclostratigraphic and sequence stratigraphic context.

682

683 **Acknowledgments**

684 Franciane Le Quellec and Julien Le Quellec at the Réserve Naturelle de Saint-Barthélemy
685 (resnatbarth@wanadoo.fr) are gratefully acknowledged for providing practical and logistical
686 support. The authors wish to thank Eric François and Pierre Soudet for taxonomic identification
687 of echinoid fossils. We are grateful to Sedimentary Geology associate editor and to an
688 anonymous reviewer for their contribution towards improving this manuscript.

689

690 **References**

691

692 Adams, C.G., 1965. The foraminifera and stratigraphy of the Melinau Limestone, Sarawak, and
693 its importance in Tertiary correlation. Quarterly Journal of the Geological Society of London
694 121, 283-338.

- 695
- 696 Afzal, J., Williams, M., Leng, M.J., Aldridge, R.J., 2011. Dynamic response of the shallow
697 marine benthic ecosystem to regional and pan-Tethyan environmental change at the
698 Paleocene Eocene boundary. *Palaeogeography Palaeoclimatology Palaeoecology* 309, 141-
699 160.
- 700
- 701 Aguirre J., Braga J.C., Bassi D., 2017. The role of rhodoliths and rhodolith beds in the rock
702 record and their use in palaeoenvironmental reconstructions. In : Riosmena-Rodriguez R.,
703 Nelson W., Aguirre J. (Eds), *Rhodolith/maerl beds: a global perspective*. Springer-Verlag,
704 Berlin, special volume, pp. 105-138
- 705
- 706 Allmon, W.D., 1992. Role of temperature and nutrients in extinction of turritelline gastropods:
707 Cenozoic of the northwestern Atlantic and northeastern Pacific. *Palaeogeography*
708 *Palaeoclimatology Palaeoecology* 92, 41-54.
- 709
- 710 Alve, E., 1999. Colonization of new habitats by benthic foraminifera: a review. *Earth-Science*
711 *Reviews* 46, 167-185.
- 712
- 713 Barattolo, F., Bassi, D., Romano, R., 2007. Upper Eocene larger foraminiferal-coralline algal
714 facies from the Klokova Mountain (southern continental Greece). *Facies* 53, 361-375.
- 715
- 716 Bassi, D., 1998. Coralline algal facies and their palaeoenvironment in the Late Eocene of
717 Northern Italy (Calcare di Nago, Trento). *Facies* 39, 179-202.
- 718

- 719 Bassi, D., 2005. Larger foraminiferal and coralline algal facies in an Upper Eocene storm-
720 influenced, shallow-water carbonate platform (Colli Berici, north-eastern Italy).
721 *Palaeogeography Palaeoclimatology Palaeoecology* 226, 17-35.
722
- 723 Beavington-Penney, S.J., 2004. Analysis of the effects of abrasion on the tests of
724 *Palaeonummulites venosus*: implications for the origin of nummulithoclastic sediments.
725 *Palaios* 19, 143-155.
726
- 727 Beavington-Penney, S.J., Racey, A., 2004. Ecology of extant nummulitids and other larger
728 benthic foraminifera: applications in palaeoenvironmental analysis. *Earth-Science Reviews*
729 67, 219-265.
730
- 731 Berra, F., Carminati, E., 2012. Differential compaction and early rock fracturing in high-relief
732 carbonate platforms : numerical modelling of a Triassic case study (Esino limestone, central
733 southern Alps, Italy). *Basin Research* 24, 598-614.
734
- 735 Bouysse, P., Westercamp, D., Andreieff, P., 1990. The Lesser Antilles island arc. In: Moore, J.C.,
736 Mascle, A. et al. (Eds.) *Proceedings of ODP Science Research* 110, pp. 29-44.
737
- 738 Burchette, T.P., Wright, V.P., 1992. Carbonate ramp depositional systems. *Sedimentary Geology*
739 79, 3-57.
740
- 741 Braga, J.C., Martín, J.M., 1988. Neogene coralline-algal growthforms and their
742 palaeoenvironments in the Almanzora River Valley (Almeria S.E. Spain). *Palaeogeography*

- 743 Palaeoclimatology Palaeoecology 67, 285-303.
- 744
- 745 Braga, J.C., Aguirre, J., 2001. Coralline algal assemblages in Upper Neogene reef and temperate
746 carbonates in southern Spain. *Palaeogeography Palaeoclimatology Palaeoecology* 175, 27-
747 41.
- 748
- 749 Braga, J.C., Vescogni, A., Bosellini, F.R., Aguirre, J., 2009. Coralline algae (Corallinales,
750 Rhodophyta) in western and central Mediterranean Messinian reefs. *Palaeogeography*.
751 *Palaeoclimatology Palaeoecology* 275, 113-128.
- 752
- 753 Brasier, M.D., 1995a. Fossil indicators of nutrient levels. 1. Eutrophication and climate change.
754 In: Bosence, D.W.J., Allison, P.A. (Eds.), *Marine Palaeoenvironmental Analysis from*
755 *Fossils*, Geological Society of London Special Publication 83, pp. 113-132.
- 756
- 757 Brasier, M.D., 1995b. Fossil indicators of nutrient levels. 2. Evolution and extinction in relation
758 to oligotrophy. In: Bosence, D.W.J., Allison, P.A. (Eds.), *Marine Palaeoenvironmental*
759 *Analysis from Fossils*, Geological Society of London Special Publication 83, pp. 133-150.
- 760
- 761 Burton, L.M., 2004. Carbonate–siliciclastic Interactions; Tertiary Examples from Spain. PhD
762 Thesis, University of Durham, UK, 396 p.
- 763
- 764 Carannante, G., Esteban, M., Milliman, J.D., Simone, L., 1988. Carbonate lithofacies as
765 paleolatitude indicators: problems and limitations. *Sedimentary Geology* 60, 333-346.
- 766

- 767 Caron, V., 2011. Contrasted textural and taphonomic properties of high-energy wave deposits
768 cemented in beachrocks (St. Bartholomew Island, French West Indies). *Sedimentary*
769 *Geology* 237, 189-208.
770
- 771 Caron, V., Nelson, C.S., Kamp, P.J.J., 2004. Contrasted carbonate depositional systems for
772 Pliocene cool-water limestones cropping out in central Hawke's Bay, New Zealand. *New*
773 *Zealand journal of Geology and Geophysics* 47, 697-717.
774
- 775 Christ, N., Immenhauser, A., Amour, F., Mutti, M., Tomás, S., Always, R., Kabir, L., 2012.
776 Characterization and interpretation of discontinuity surfaces in a Jurassic ramp setting (High
777 Atlas, Morocco). *Sedimentology* 59, 249-290.
778
- 779 Christman, R.A., 1953. Geology of St. Bartholomew, St. Martin, and Anguilla, Lesser Antilles.
780 *Bulletin of the Geological Society of America* 6, 65-96.
781
- 782 Clari, P.A., Dela Pierre, F., Martire, L., 1995. Discontinuities in carbonate successions:
783 identification, interpretation and classification of some Italian examples. *Sedimentary*
784 *Geology* 100, 97-121.
785
- 786 Cosovic, V., Drobne, K., Moro, A., 2004. Paleoenvironmental model for Eocene foraminiferal
787 limestones of the Adriatic carbonate platform (Istrian Peninsula). *Facies* 50, 61-75.
788
- 789 Dashtgard, S.E., Gingras, M.K., Pemberton, S.G., 2008. Grain-size controls on the occurrence of
790 bioturbation. *Palaeogeography Palaeoclimatology Palaeoecology* 257, 224-243.

- 791
- 792 Donovan, S.K., Rowe, D.-A.C., 2000. Spatangoid echinoids from the Eocene of Jamaica. Journal
793 of Paleontology 74, 654-661.
- 794
- 795 Dorobek, S.L., 2008. Carbonate-platform facies in volcanic-arc settings: Characteristics and
796 controls on deposition and stratigraphic development. Geological Society of America
797 Special Papers 436, 55-90.
- 798
- 799 Dumas, S., Arnott, R.C.W., 2006. Origin of hummocky and swaley cross-stratifications. The
800 controlling influence of unidirectional current strength and aggradation rate. Geology 34,
801 1073-1076.
- 802
- 803 Embry, A.F., Klovan, J.E., 1971. A late Devonian reef tract on northeastern Banks Island.
804 N.W.T. Bulletin of Canadian Petroleum Geology 19, 730-781.
- 805
- 806 Freiwald, A., 1995. Sedimentological and biological aspects in the formation of branched rhodoliths
807 in northern Norway. Beiträge zur Paläontologie 20, 7-19.
- 808
- 809 Gaillard, C., 1983. Les biohermes à spongiaires et leur environnement dans l'Oxfordien du Jura
810 méridional. Document du Laboratoire de Géologie de Lyon 90, 515 pp.
- 811
- 812 Geel, T., 2000. Recognition of stratigraphic sequences in carbonate platform and slope deposits:
813 empirical models based on microfacies analysis of Palaeogene deposits in southeastern
814 Spain. Palaeogeography Palaeoclimatology Palaeoecology 155, 211-238.

- 815
- 816 Gradstein, F.M, Ogg, J.G., Schmitz, M.D., et al., 2012. The Geologic Time Scale 2012: Boston,
817 USA, Elsevier, DOI: 10.1016/B978-0-444-59425-9.00004-4
- 818
- 819 Halfar, J., Godinez-Orta, L., Mutti, M., Valdez-Holguin, J.E., Borges, J.M., 2004. Nutrient and
820 temperature controls on modern carbonate production: An example from the Gulf of
821 California, Mexico. *Geology* 32, 213-216.
- 822
- 823 Hallock, P., 1985. Why are larger foraminifera large? *Paleobiology* 11, 195-208.
- 824
- 825 Hallock, P., 1987. Fluctuations in the trophic resource continuum: a factor in global diversity
826 cycles? *Palaeoceanography* 2, 457-471.
- 827
- 828 Hallock, P., 2001. Coral reefs, carbonate sedimentation, nutrients, and global change. In: Stanley,
829 G.D. (Ed.), *The History and Sedimentology of Ancient Reef Ecosystems*, Amsterdam
830 (Kluwer), pp. 387-427.
- 831
- 832 Hallock, P., Glenn, E.C., 1986. Larger foraminifera: a tool for palaeoenvironmental analysis of
833 Cenozoic depositional facies. *Palaios*, 1, 55-64.
- 834
- 835 Hallock, P., Schlager, W., 1986. Nutrient excess and the demise of coral reefs and the demise of
836 coral reefs and carbonate platforms. *Palaios* 1, 389-398.
- 837
- 838 Hallock, P., Sheps, K., Chapronière, G., Howell, M, 2006. Larger benthic foraminifers of the

- 839 marion plateau, northeastern Australia (ODP leg 194): comparison of faunas from bryozoan
840 (sites 1193 and 1194) and red algal (sites 1196-1198) dominated carbonate platforms. In:
841 Anselmetti, F.S., Isern, A.R., Blum, P., Betzler, C. (Eds.), Proceedings of the Ocean Drilling
842 Program, Scientific Results 194, pp. 1-31.
- 843
- 844 Harvey, A.S., Broadwater, S.T., Woelkerling, W.J., Mitrovski, P.J., 2003. *Choreonema*
845 (Corallinales, Rhodophyta): 18S rDNA phylogeny and resurrection of the Hapalidiaceae for
846 the subfamilies Choreonematoideae, Austrolithoideae, and Melobesioideae. *Journal of*
847 *Phycology* 39, 988-998.
- 848
- 849 Hayton, S., Nelson, C.S., Hood, S.D., 1995. A skeletal assemblage classification system for non-
850 tropical carbonate deposits based on New Zealand Cenozoic limestones. *Sedimentary*
851 *Geology* 100, 123-141.
- 852
- 853 Heikoop, J.M., Tsujita, C.J., Heikoop, C.E., Risk, M., Dickin, A.P., 1996. Effects of volcanic
854 ashfall recorded in ancient marine benthic communities: comparison of a nearshore and an
855 offshore environment. *Lethaia* 29, 125-139.
- 856
- 857 Hendry, J.P., Taberner, C., Marshall, J.D., Pierre, C., Carey, P.F., 1999. Coral reef diagenesis
858 records pore-fluid evolution and paleohydrology of a siliciclastic basin margin succession
859 (Eocene South Pyrenean foreland basin, northeastern Spain). *Geological Society of America*
860 *Bulletin* 111, 395-411.
- 861
- 862 Hillgärtner, H., 1998. Discontinuity surfaces on a shallow marine carbonate platform (Berriasian–

- 863 Valanginian, France and Switzerland). *Journal of Sedimentary Research* 68, 1093-1108.
864
- 865 Hinchey, E., Schaffner, L., Hoar, C., Vogt, B., Batte, L., 2006. Responses of estuarine benthic
866 invertebrates to sediment burial: the importance of mobility and adaptation. *Hydrobiologia*
867 556, 85-98.
868
- 869 Hohenegger, J., 2009. Functional shell geometry of symbiont-bearing foraminifera. *Research*
870 *Galaxea, Journal of Coral Reef Studies* 11, 81-89.
871
- 872 Hohenegger, J., Yordanova, E., 2001. Displacement of larger Foraminifera at the western slope
873 of Motobu Peninsula (Okinawa, Japan). *Palaios* 16, 53-72
874
- 875 Hohenegger, J., Yordanova, E., Hatta, A., 2000. Remarks on West Pacific Nummulitidae
876 (Foraminifera). *Journal of Foraminiferal Research* 30(1), 3-28.
877
- 878 Hottinger, L., 1983. Processes determining the distribution of larger foraminifera in space and
879 time. *Utrecht Micropaleontology Bulletin* 30, 239-253.
880
- 881 Hottinger, L., 1997. Shallow benthic foraminiferal assemblages as signals for depth of their
882 deposition and their limitations. *Bulletin de la Société Géologique de France* 168, 491-505.
883
- 884 Hughes, T.P., 1987. Skeletal density and growth form of corals. *Marine Ecology – Progress*
885 *Series* 35, 259-266.
886

- 887 Iryu, Y., Nakamori, T., Matsuda, S., Abe, O., 1995. Distribution of marine organisms and its
888 geological significance in the modern reef complex of the Ryukyu Islands. *Sedimentary*
889 *Geology* 99, 243-258.
890
- 891 James, N.P., 1997. The cool-water carbonate depositional realm. In: James, N.P., Clarke, J.
892 (Eds.), *Cool-Water Carbonates*. SEPM Special Publication 56, pp. 1-20.
893
- 894 Jeans, C.V., Wray, D.S., Merriman, R.J., Fisher, M.J., 2000. Volcanogenic clays in Jurassic and
895 Cretaceous strata of England and the North Sea Basin. *Clay Minerals* 35, 25-55.
896
- 897 Kanazawa, K., 1992. Adaptation of test shape for burrowing and locomotion in spatangoid
898 Echinoids. *Paleontology* 35, 733-750.
899
- 900 Kier, P.M., 1984. Fossil Spatangoid Echinoids of Cuba. *Smithsonian Contribution to*
901 *Paleobiology* 55, 336 pp.
902
- 903 Knoll, K., Chamberlain, R.B., Chamberlain, J.A. Jr., 2017. Escape burrowing of modern
904 freshwater bivalves as a paradigm for escape behavior in the Devonian bivalve *Archanodon*
905 *catskillensis*. *Geosciences* 7, 37 pp.
906
- 907 Langer, M.R., Hottinger, L., 2000. Biogeography of selected larger foraminifera.
908 *Micropaleontology* 46, 105-126.
909
- 910 Lees, A., 1975. Possible influence of salinity and temperature on modern shelf carbonate

- 911 sedimentation. *Marine Geology* 19, 159-198.
- 912
- 913 Lees, A., Buller, A.T., 1972. Modern temperate water and warm water shelf carbonate sediments
914 contrasted. *Marine Geology* 13, M67–M73.
- 915
- 916 Lokier, S.W., Wilson, M.E.J., Burton, L.M., 2009. Marine biota response to clastic sediment
917 influx: a quantitative approach. *Palaeogeography Palaeoclimatology Palaeoecology* 175,
918 249-272.
- 919
- 920 Loucks, R.G., Moody, R.T.J., Bellis, J.K., Brown, A.A., 1998. Regional depositional setting and
921 pore network systems of the El Garia Formation (Metlaoui Group, Lower Eocene), offshore
922 Tunisia. In: Macgregor, D.S., Moody, R.T.J., Clark-lowes, D.D. (Eds.), *Petroleum geology*
923 *of North Africa*, Geological Society of London Special Publication 132, pp. 355-374.
- 924
- 925 Lukasik, J.J., James, N.P., 2003. Deepening-upward subtidal cycles, Murray Basin, South
926 Australia. *Journal of Sedimentary Research* 73, 653-671.
- 927
- 928 Lund, M., Davies, P.J., Braga, J.C., 2000. Coralline algal nodules off Fraser Island eastern
929 Australia. *Facies* 42, 25-34.
- 930
- 931 Marrack, E.C., 1999. The relationship between water motion and living rhodolith beds in the
932 southwestern Gulf of California, Mexico. *Palaios* 14, 159-171.
- 933
- 934 Mitchell, S.F., 2004. Lithostratigraphy and palaeogeography of the White Limestone Group.

935 Cainozoic Research 3, 5-29.

936

937 Mitchell, S.F., 2013. Stratigraphy of the White Limestone of Jamaica. Bulletin de la Société
938 Géologique de France 184, 111-118.

939

940 Murray, J.W., 1991. Ecology and distribution of benthic foraminifera. In: Lee, J.J., Anderson,
941 R.O. (Eds.), Biology of Foraminifera. Academic Press, London, pp. 221-284.

942

943 Nalin, R., Massari, F., 2009. Facies and stratigraphic anatomy of a temperate carbonate sequence
944 (Capo Colonna terrace, Late Pleistocene, Southern Italy). Journal of Sedimentary Research
945 79, 210-225.

946

947 Nalin, R., Nelson, C.S., Basso, D., Massari, F., 2007. Rhodolith-bearing limestones as
948 transgressive marker beds: fossil and modern examples from North Island, New Zealand.
949 Sedimentology 55, 249-274.

950

951 Nebelsick, J.H., Bassi, D., 2000. Diversity, growth forms and taphonomy: key factors controlling
952 the fabric of coralline algae dominated shelf carbonates. In: Insalaco, E. Skelton, P.W.,
953 Palmer, T.J. (Eds.), Carbonate Platform Systems: components and interactions, Geological
954 Society of London Special Publication 178, pp. 89-107.

955

956 Nebelsick J.H., Rasser M., Bassi D. 2005. Facies dynamics in Eocene to Oligocene circumalpine
957 carbonates. Facies, 51, 197-216.

958

- 959 Pandolfi, J.M., Tudhope, A.W., Burr, G., Chapell, J., Edinger, E., Frey, M., Steneck, R., Sharma,
960 C., Yeates. A., Jennions, M., Lescinsky, H., Newton. A., 2006. Mass mortality following
961 disturbance in Holocene coral reefs from Papua New Guinea. *Geology* 34, 949-952.
962
- 963 Payros, A., Pujalte, V., Tosquella, J., Orue-Etxebarria, V., 2010. The Eocene storm-dominated
964 foralgal ramp of the western Pyrenees (Urbasa–Andia Formation): An analogue of future
965 shallow-marine carbonate systems? *Sedimentary Geology* 228, 184-204.
966
- 967 Perry, C.T., 1998. Grain susceptibility to the effects of microboring: implications for the
968 preservation of skeletal carbonates: *Sedimentology* 45, 39-51.
969
- 970 Pomar, L., 2001. Ecological control of sedimentary accommodation: evolution from carbonate
971 ramp to rimmed shelf, Upper Miocene, Balearic Islands. *Palaeogeography Palaeoclimatology*
972 *Palaeoecology* 175, 249-272.
973
- 974 Pomar, L., Brandano, M., Westphal, H., 2004. Environmental factors influencing skeletal grain
975 sediment associations: a critical review of Miocene examples from the western
976 Mediterranean. *Sedimentology* 51, 627-651.
977

- 978 Puga-Bernabéu, Á., Martín, J.M., Braga, J.C., Sánchez-Almazo, I.M., 2010. Downslope-
979 migrating sandwaves and platform-margin clinofolds in a current-dominated, distally
980 steepened temperate-carbonate ramp (Guadix Basin, Southern Spain). *Sedimentology* 57,
981 287-311.
- 982
- 983 Rasser, M.W., 2000. Coralline red algal limestones of the Late Eocene Alpine Foreland Basin in
984 Upper Austria: component analysis, facies and paleoecology. *Facies* 42, 59-92.
- 985
- 986 Rasser, M.W., Piller, W.E., 1999. Application of neontological taxonomic concepts to Late
987 Eocene coralline algae (Rhodophyta) of the Austrian Molasse Zone. *Journal of*
988 *Micropalaeontology* 18, 67-80.
- 989
- 990 Reading, H.G., 1996. *Sedimentary environments: Processes, facies and stratigraphy*. Blackwell
991 Science, Oxford.
- 992
- 993 Reuter, M., Piller, W.E., 2011. Volcaniclastic events in coral reef and seagrass environments:
994 evidence for disturbance and recovery (Middle Miocene, Styrian Basin, Austria). *Coral*
995 *Reefs* 30, 889-899.
- 996
- 997 Reuter, M., Piller, W.E., Erhart, C., 2012. A Middle Miocene carbonate platform under silici-
998 volcaniclastic sedimentation stress (Leitha Limestone, Styrian Basin, Austria) - Depositional
999 environments, sedimentary evolution and palaeoecology. *Palaeogeography*
1000 *Palaeoclimatology Palaeoecology* 350-352, 198-211.

- 1001
- 1002 Rusciadelli, G., Di Simone, S., 2007. Differential compaction as control on depositional
1003 architectures across the Maiella carbonate platform margin (central Appenines, Italy).
1004 *Sedimentary Geology* 196, 133- 155.
- 1005
- 1006 Schlager, W., 1989. Drowning unconformities on carbonate platforms. In: Crevello, P.D.,
1007 Wilson, J.L., Sarg, J.F., Read, J.F. (Eds.), *Controls on Carbonate Platforms and Basins*
1008 *Development. SEPM Special Publication* 44, pp. 15-25.
- 1009
- 1010 Sola, F., Braga, J.C., Aguirre, J., 2013. Hooked and tubular coralline algae indicate seagrass beds
1011 associated to Mediterranean Messinian reefs (Poniente Basin, Almería, SE Spain).
1012 *Palaeogeography Palaeoclimatology Palaeoecology* 374, 218-229.
- 1013
- 1014 Tinterri, R., 2011. Combined flow sedimentary structures and the genetic link between
1015 sigmoidal- and hummocky- cross stratification. *GeoActa* 10, 43-85.
- 1016
- 1017 Tomascik, T., van Woesik, R., Mah, A.J., 1996. Rapid coral colonization of a recent lava flow
1018 following a volcanic eruption, Banda Islands, Indonesia. *Coral Reefs* 15, 169-175.
- 1019
- 1020 Trofimovs, J., Amy, L., Boudon, G., Deplus, C. Doyle, E., Fournier, N., Hart, M.B., et al. 2006.
1021 Submarine pyroclastic deposits formed at the Soufrière Hills volcano, Montserrat (1995-
1022 2003): What happens when pyroclastic flows enter the ocean? *Geology* 34, 549-552.
- 1023
- 1024 Vecchio, E., Hottinger, L., 2007. Agglutinated conical foraminifera from the Lower-Middle

- 1025 Eocene of the Trentinara Formation (southern Italy). *Facies* 53, 509-533.
- 1026
- 1027 Vroom, P.S., Zgliczynski, B.J., 2011. Effects of volcanic ash deposits on four functional groups
1028 of a coral reef. *Coral Reefs* 30, 1025-1032.
- 1029
- 1030 Westercamp, D., Andreieff, P., 1983a. St-Barthélémy et ses îlets, Antilles françaises:
1031 stratigraphie et evolution magmato-structurale. *Bulletin de la Société Géologique de France*
1032 25, 873-883.
- 1033
- 1034 Westercamp, D., Andreieff, P., 1983b. Saint-Barthélémy et ses îlets - Carte géologique à
1035 1/20000: Notice explicative. Service Géologique National, Orléans, France, 38 pp.
- 1036
- 1037 Wilson, M.E.J., 2002. Cenozoic carbonates in Southeast Asia: implications for equatorial
1038 carbonate development. *Sedimentary Geology* 147, 295-328.
- 1039
- 1040 Wilson, M.E.J., Bosence, D.W.J., Limbong, A., 2000. Tertiary syntectonic carbonate platform
1041 development in Indonesia. *Sedimentology* 47, 395-419.
- 1042
- 1043 Wilson, M.E.J., Lokier, S.W., 2002. Siliciclastic and volcanoclastic influences on equatorial
1044 carbonates: insights from the Neogene of Indonesia. *Sedimentology* 49, 583-601.
- 1045
- 1046 Wilson, M.E.J., Vecsei, A., 2005. The apparent paradox of abundant foramol facies in low
1047 latitudes: their environmental significance and effect on platform development. *Earth-*
1048 *Science Reviews* 69, 133-168.

1049
1050 Zamagni, J., Mutti, M., Kosir, A., 2008. Evolution of shallow benthic communities during the
1051 Late Paleocene-earliest Eocene transition in the Northern Tethys (SW Slovenia). *Facies* 54,
1052 25-43.

1053

1054 **Figure captions**

1055

1056 Fig. 1. (A) Location of St. Bartholomew relative to the main geological features of the Lesser
1057 Antilles in the eastern Caribbean. (B) Simplified lithostratigraphy of the Middle Eocene of St
1058 Bartholomew showing the main volcanic and limestone units. Not to scale. (C) Map showing
1059 outcropping distribution of limestone units, key stratigraphical sections (arrowed) and inferred
1060 location of eruptive centers (based on Westerkamp and Anfreieff, 1983b).

1061

1062 Fig. 2. Examples of stratigraphic columns logged in the studied Eocene limestones. See Fig. 1 for
1063 locations.

1064

1065 Fig. 3. Paleoecological modes of the most frequent irregular echinoids found in the St.
1066 Bartholomew middle Eocene limestones (based on Kanazawa, 1992).

1067

1068 Fig. 4. Taphonomic grading system established for several skeletal categories. The scale of
1069 fragmentation features for benthic foraminifers derives from that proposed by Beavington-
1070 Penney (2004). The scale of mechanical alteration for calcareous green algae is modified from
1071 Caron (2011). The importance of test infestation follows the visual chart presented in Perry
1072 (1998).

1073

1074 Fig. 5. Field photographs of volcanoclastic deposits from various locations (see Fig. 1). (A, B)

1075 Coarse volcanoclastic breccia containing heterometric angular clasts, ranging in size from gravel

1076 to boulder (white arrow in A), tapering limestone clasts (black arrow in A) and coral heads

1077 (arrowed in B). es: erosional surface. Location: Anse Chauvette. (C) Superposed fining-upwards

1078 dm- to m-thick pyroclastic beds exhibiting from base (arrowed) to top an erosional surface (relief

1079 <5 cm), a conglomeratic layer grading into planar-bedded gravels and sands. Anse des Cayes

1080 (Figs. 1, 12B). (D, E) Reworked hyaloclastites. Hammer: 30 cm. Location: Anse des Flamands.

1081 (F) cm- and dm-thick tabular beds of silty to sandy lapilli tuffs with wavy bases in places.

1082 Hammer: 30 cm. Location: Pointe Lézarde.

1083

1084 Fig. 6. Photomicrographs illustrating dominant microfacies in the studied deposits. (A-B) mixed

1085 microfacies Mf1, packstone containing abundant miliolids (Mi)(A) and common agglutinated

1086 conicals (dictyoconids, B). (C) Microfacies Mf3, packstone/grainstone containing echinoid plates

1087 (Ec), peloids and micritized grains (Micr). (D) Microfacies Mf5 (see Table 1). (E) Microfacies

1088 facies DaMi, wackestone/packstone characterized by dasycladal algal debris (Da), miliolids (Mi)

1089 and meliobesoids (Me). (F) Example of larger benthic foraminiferal - rhodolith photozoan

1090 microfacies LfRh. (G, H) Example of photozoan microfacies LfCa, packstone containing abraded

1091 and fragmented (arrowed) amphisteginids (G) and (H) grainstone showing bioclasts of

1092 orthophragminid (Or) and echinoid (Ec). (I) Example of echinoid facies association EcF,

1093 grainstone with echinoid plate (Ec) and mollusk (M) fragments.

1094

1095 Fig. 7. Examples of coral reef buildups. For locations see Figure 1. (A) Meter-sized lenticular

1096 reef possibly exhibiting several growth-phases (arrows), each one being laterally correlated to

1097 limestone beds. Location: Anse des Cayes. (B) Massive coral buildup, 8 m thick (dashed line),
1098 interpreted as an isolated coral bioherm. Coral heads are in living position in the upper part of the
1099 structure whereas it is not as clear in its lower part. Location: Pain de sucre.

1100

1101 Fig. 8. Hypothetical paleoenvironmental reconstruction and depositional profile of the ramp
1102 attached to submarine volcanoes for the middle Eocene limestones of St. Bartholomew.

1103

1104 Fig. 9. Anse des Cayes section (Limestone unit 3 - see Fig. 1 for location and Fig. 12 for field
1105 photograph) showing the interplay between volcanoclastic and carbonate sedimentation. t. arr. :
1106 temporarily arrested.

1107

1108 Fig. 10. Consequences of the onset of volcanic activity on inner- to middle-ramp carbonate
1109 factories. A) Demise due to burial following emplacement of coarse-grained pyroclastic deposits
1110 (facies Vbr and Hy; Table 1); B) Collapse due to burial by volcanic ash (facies Tu; Table 1).

1111

1112 Fig. 11. Detailed portions of lithologic logs (see Fig. 2) showing the vertical facies successions
1113 within the deposits associated with carbonate production breaks and renewal.

1114

1115 Fig. 12. Sedimentary surfaces recording interruption of carbonate production. See Figure 1 for
1116 locations. (A) Sharp contact (sc) between lagoonal facies below and sand-sized volcanoclastics
1117 above. Hammer: 30 cm. Location: Pointe Mangin. (B) Gradational contact (gc) between mixed
1118 carbonate-volcanoclastic deposits (Mf) below and cross-bedded hyaloclastites above (Hy2). The
1119 contact with the limestone unit (Lu) above is described in Figure 11E. Location: Anse des
1120 Flamands. (C, D) Burrowed omission surface (bs). Close-up view in D. Scale: 12 cm. (E)

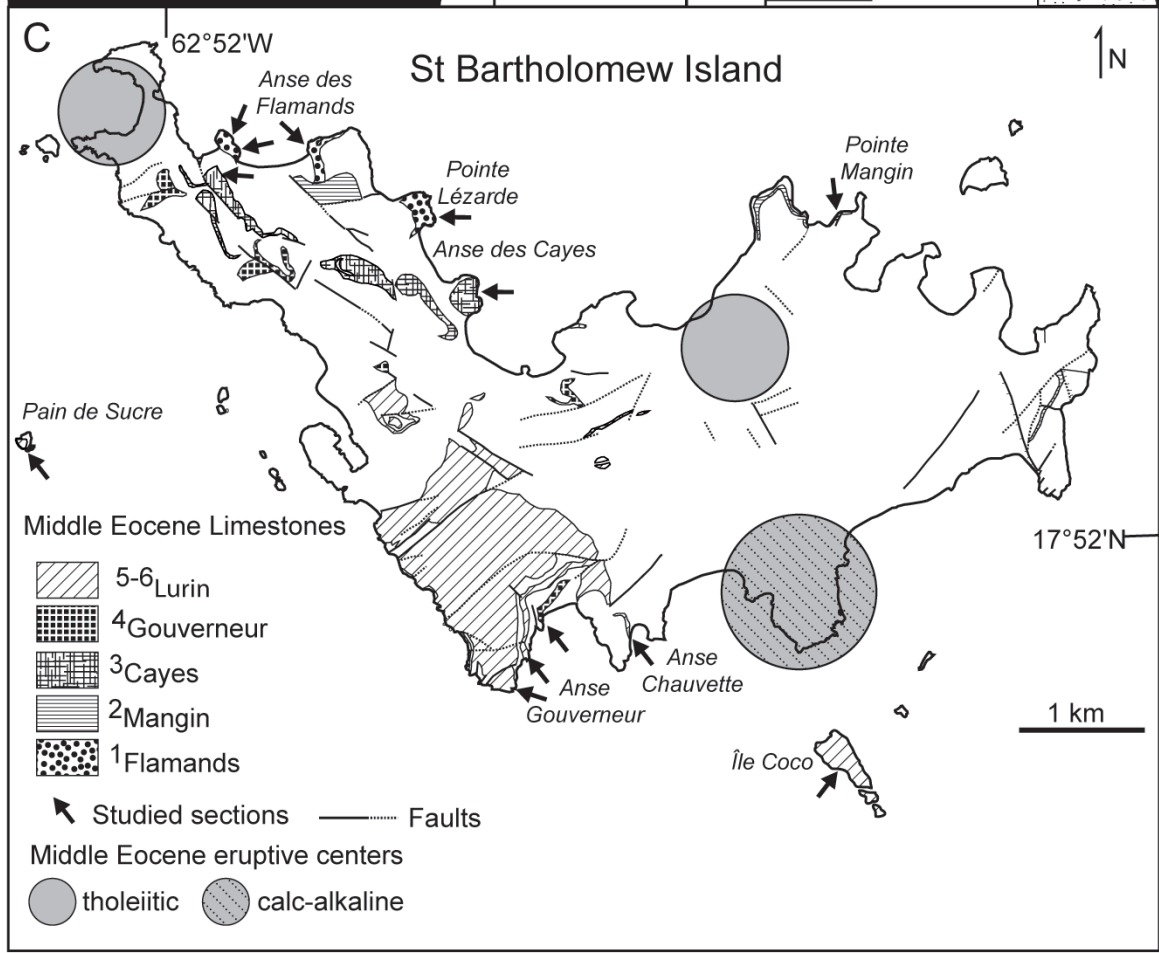
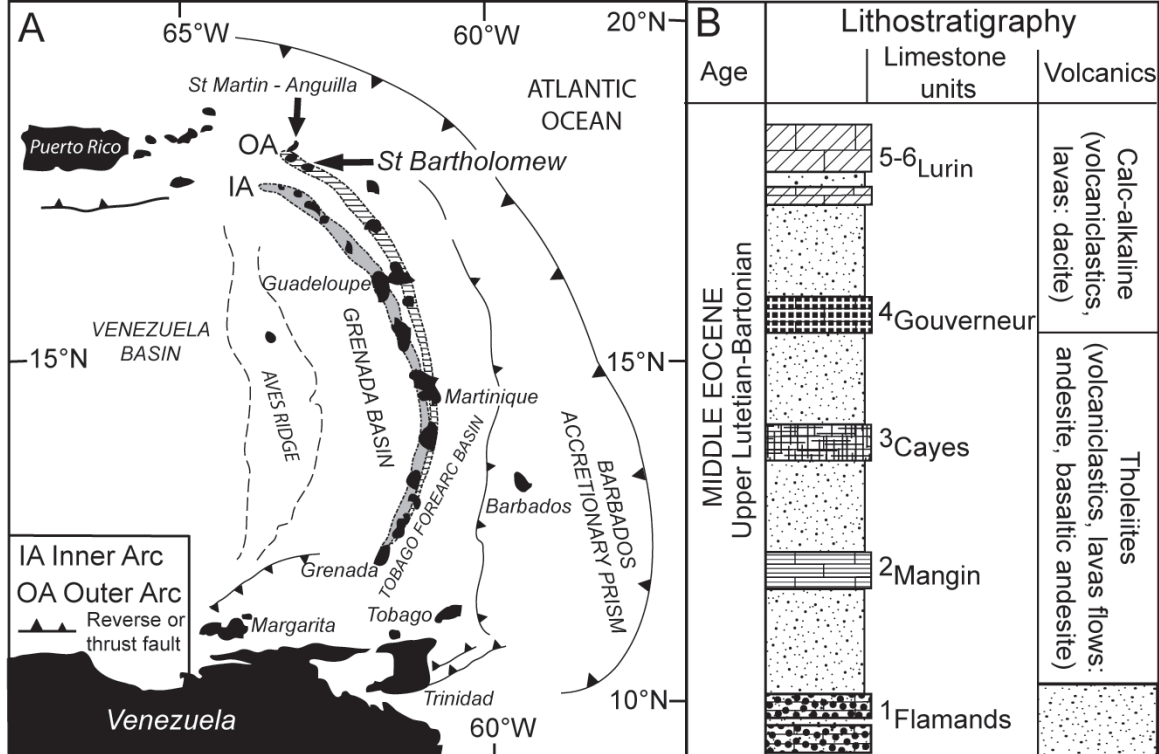
1121 Burrowed surface (bs). Iron mineralization is pervasive in the 50 cm-thick layer above. Location:
1122 Anse Gouverneur. (F) Burrowed omission surface seen in bedding plane on the right and
1123 overlying iron-stained deposit on the left. Arrow points to iron mineralization of burrow walls.
1124 Scale: 12 cm. (G) Close-up view of iron-stained deposit in E and F. Irregular echinoids (Ec) of
1125 different paleoecological modes (see text for details) are abundant together with pinnid fragments
1126 (Pi). Scale: 12 cm.

1127
1128 Fig. 13. Sedimentary surfaces recording the renewal of carbonate production after prolonged
1129 interruption due to volcanic activity. See Figure 1 for locations. (A) Sharp (sc), slightly
1130 undulating, weakly burrowed surface at volcanoclastic-carbonate boundary. Location: Anse des
1131 Cayes. (B) Lateral correlative surface seen in B. (C) Erosional surface (es) with a relief up to 10
1132 cm. From the surface, fine-grained volcanoclastic deposits below are densely bioturbated by
1133 *Thalassinoides* (See D). Location: Pointe Mangin. (D) Close up view of *Thalassinoides* burrows
1134 beneath the erosional surface in C. Scale: 12 cm. (E-F) Gradational contact (gc) from argillaceous
1135 tuffitic deposits below to well-lithified grey limestone beds above with a transitional
1136 concretionary layer in between. Close-up view in F. Scale: 20 cm. Location: Pointe Lézarde.

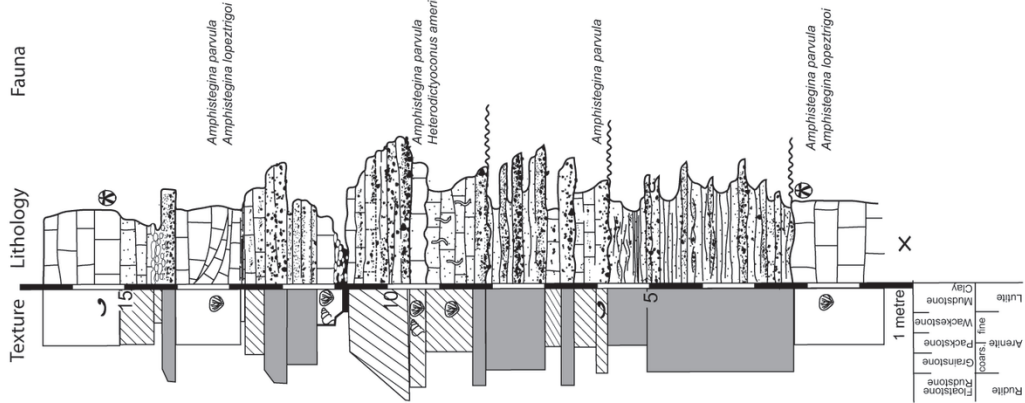
1137
1138 Table 1. Summary of facies in middle Eocene limestone units of St. Bartholomew island.
1139 Texture : 'Ms' correspond to mudstone ; 'Ws' to wackestone ; 'Ps' to packstone ; 'Gs' to
1140 grainstone ; 'Fs' to floatstone ; 'Rs' to rudstone ; 'Bs' to boudnstone ; and 'Bis' to bindstone.
1141 Taphonomy : 'l' correspond to low ; 'm' to moderate, 'h' to high degree of alteration.

1142

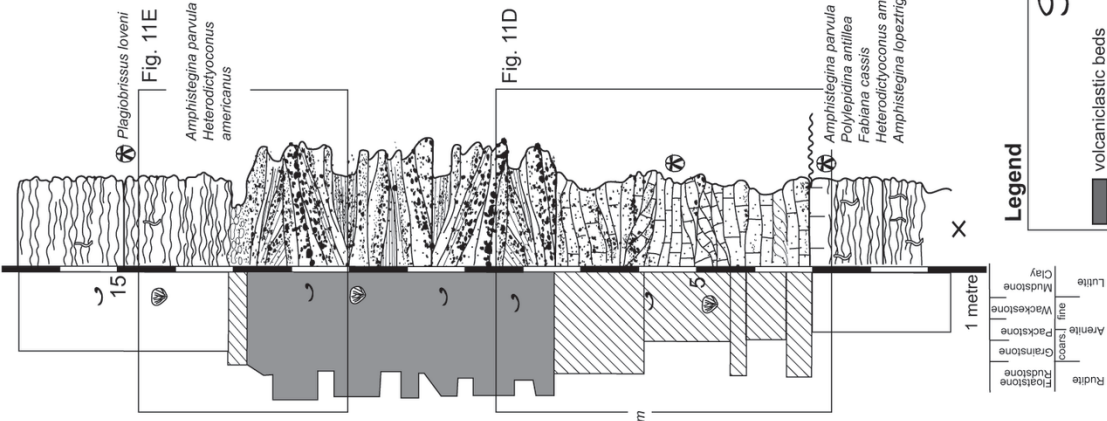
1143



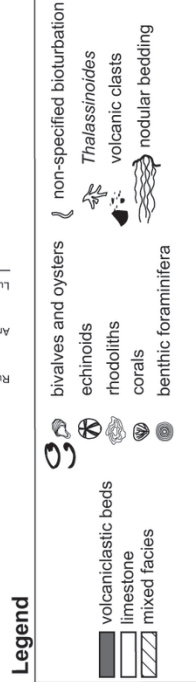
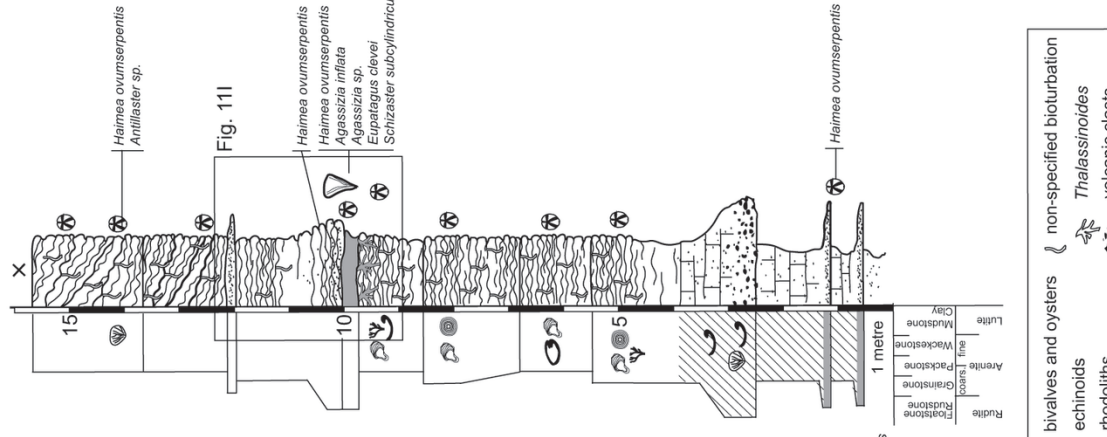
A. East Flamand
Limestone unit 1

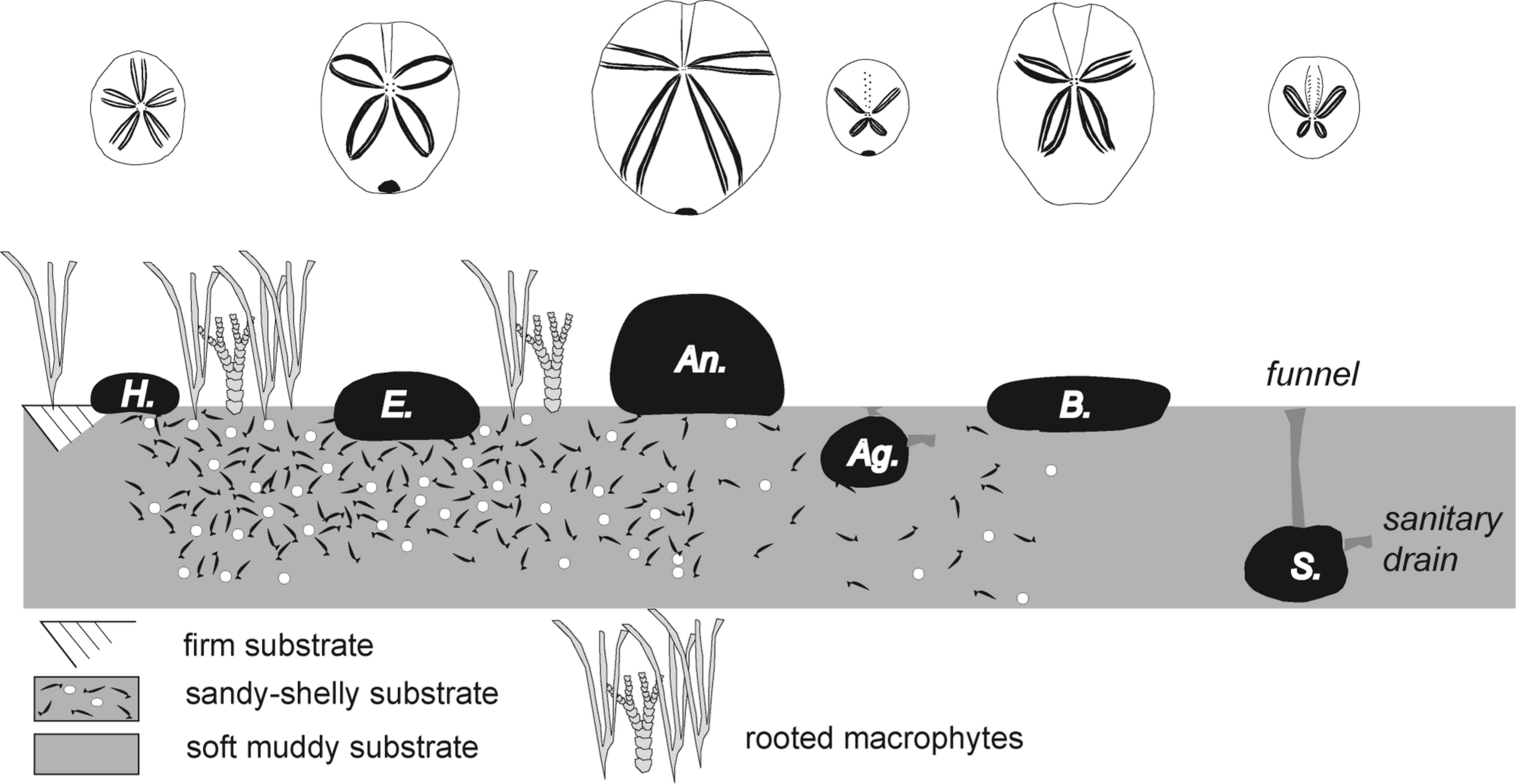


C. Pointe Lézarde
Limestone unit 1




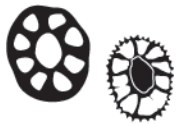














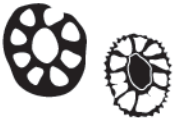




















D. Gouverneur
limestone unit 4

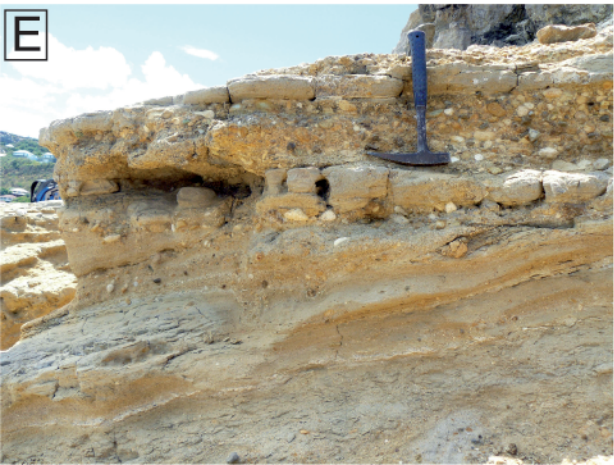


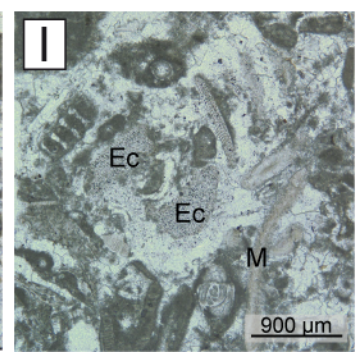
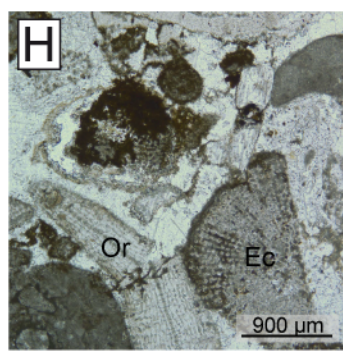
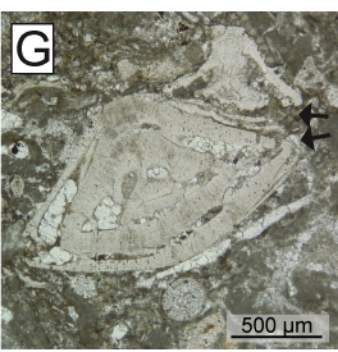
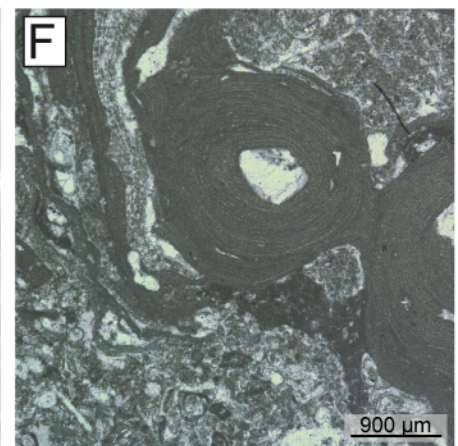
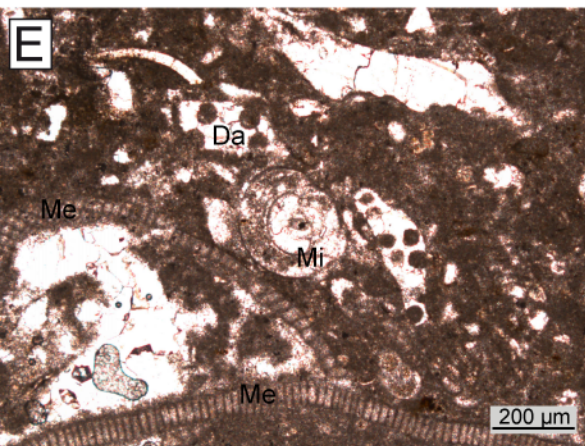
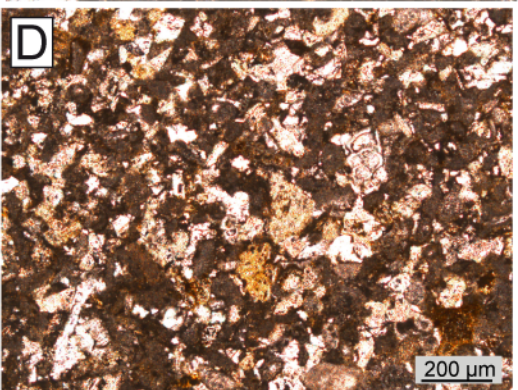
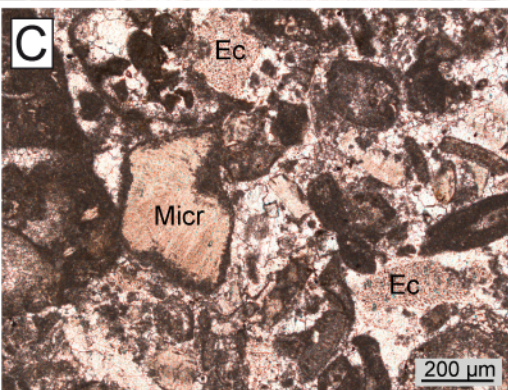
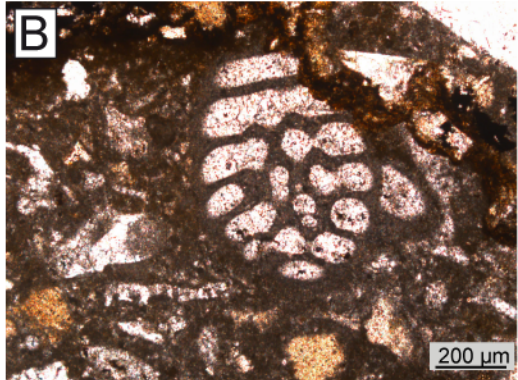
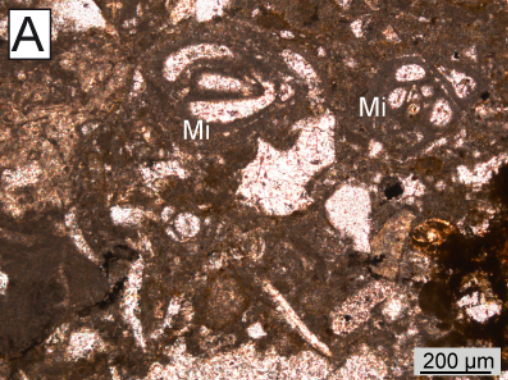


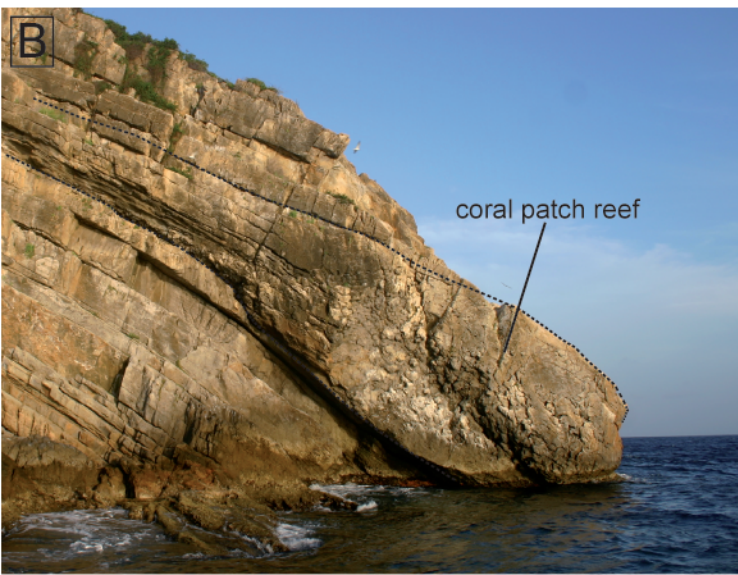
H.: *Haimea*; *E.:* *Eupatagus*; *An:* *Antillaster*; *Ag.:* *Agassizia*; *B.:* *Brissoides*; *S.:* *Schyzaster*.

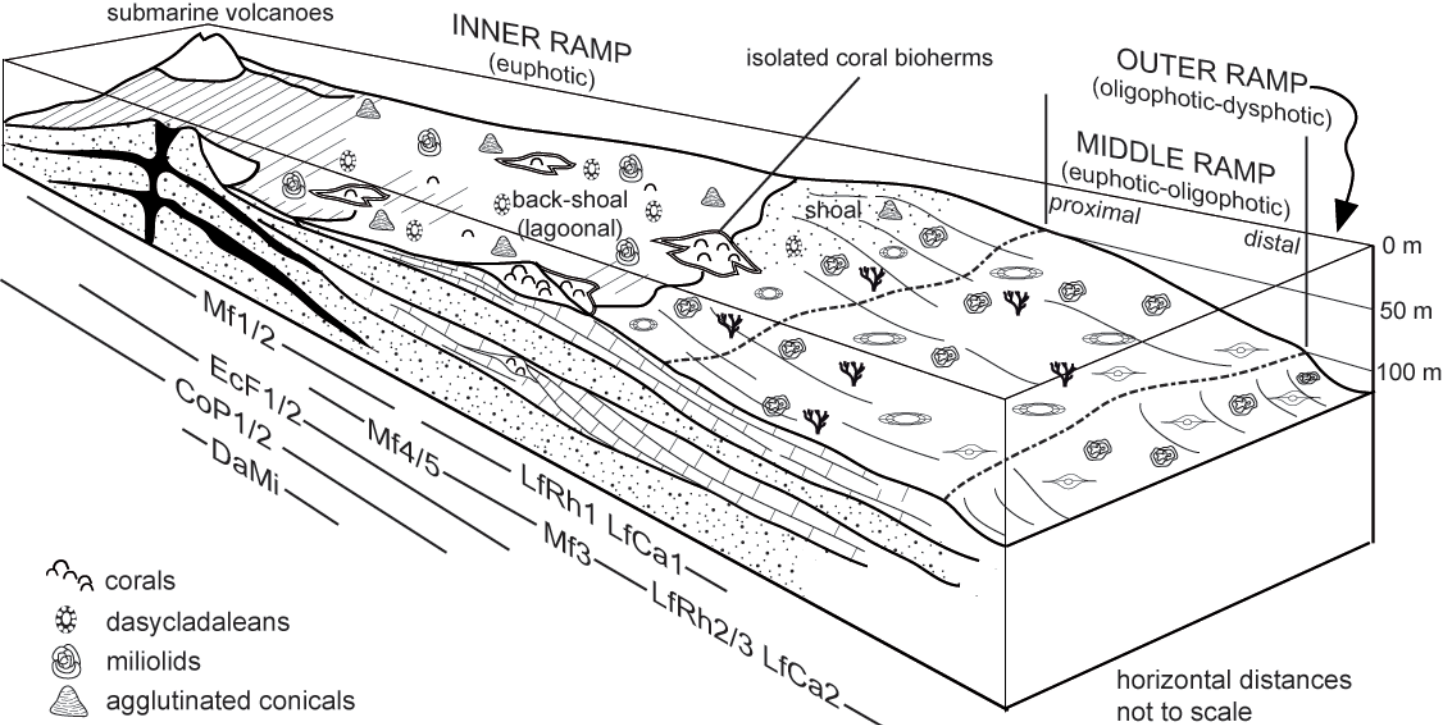
	Amph./ Numm.*	Coralline Algae	Mollusks (Bivalves)	Green Algae (Dasycladalean)	Green Algae (Halimeda)
FRAGMENTATION	Null/Low 				
	Moderate 				
	High 				
ABRASION	Low 				
	Moderate 				
	High 				

BIOEROSION	ENCRUSTATION
  Low Moderate	on one side  Moderate
  High Very high	on two sides  Moderate
* Amphisteginids: applies to Nummulitids and Lepidocylinids	multilayered  High









-  corals
-  dasycladaleans
-  miliolids
-  agglutinated conicals
-  rhodoliths
-  bryozoans
-  oblate amphoteginids and nummulitids
-  elongate nummulitids
-  orthophragminids

-  lava flow
-  volcaniclastic deposits
-  carbonate deposits
-  mixed deposits

foralgal (larger foraminifer-coralline algae photozoan): LfCa1, 2

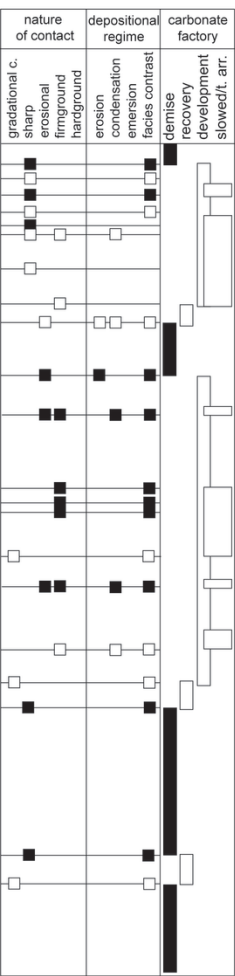
rhodalgal (rhodolith photozoan): LfRh1, 2, 3

chloralgal (dasycladacean-miliolid photozoan): Mf1, 2 - DaMi

chlorozoan (coral photozoan): CoP1, 2

echinofor (echinoid-larger foraminifer-coralline algae photozoan): EcF1,2; Mf3

foramol (larger foraminifer-mollusk photozoan): Mf4



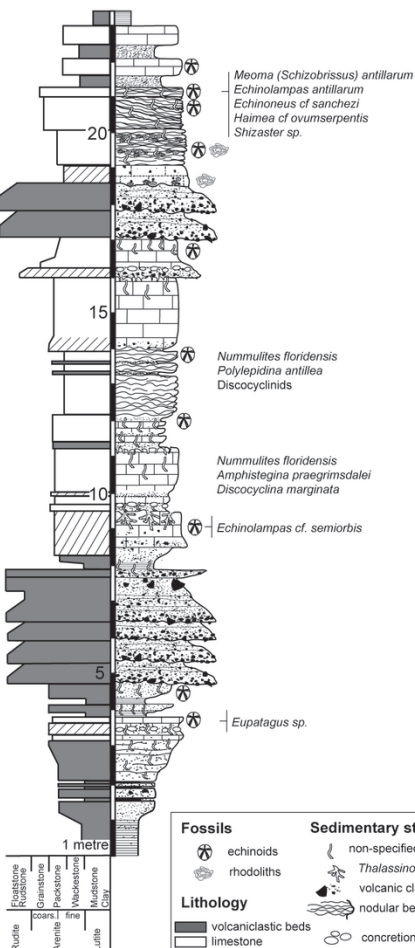
carbonate system (white)
 □ characteristics of sedimentary surface
 volcaniclastic influx (black)
 ■ characteristics of sedimentary surface

Samples

Texture

Field observations

Fauna



Legend

Fossils

- ⊗ echinoids
- ⊕ rhodoliths

Lithology

- volcaniclastic beds
- limestone
- ▨ mixed facies

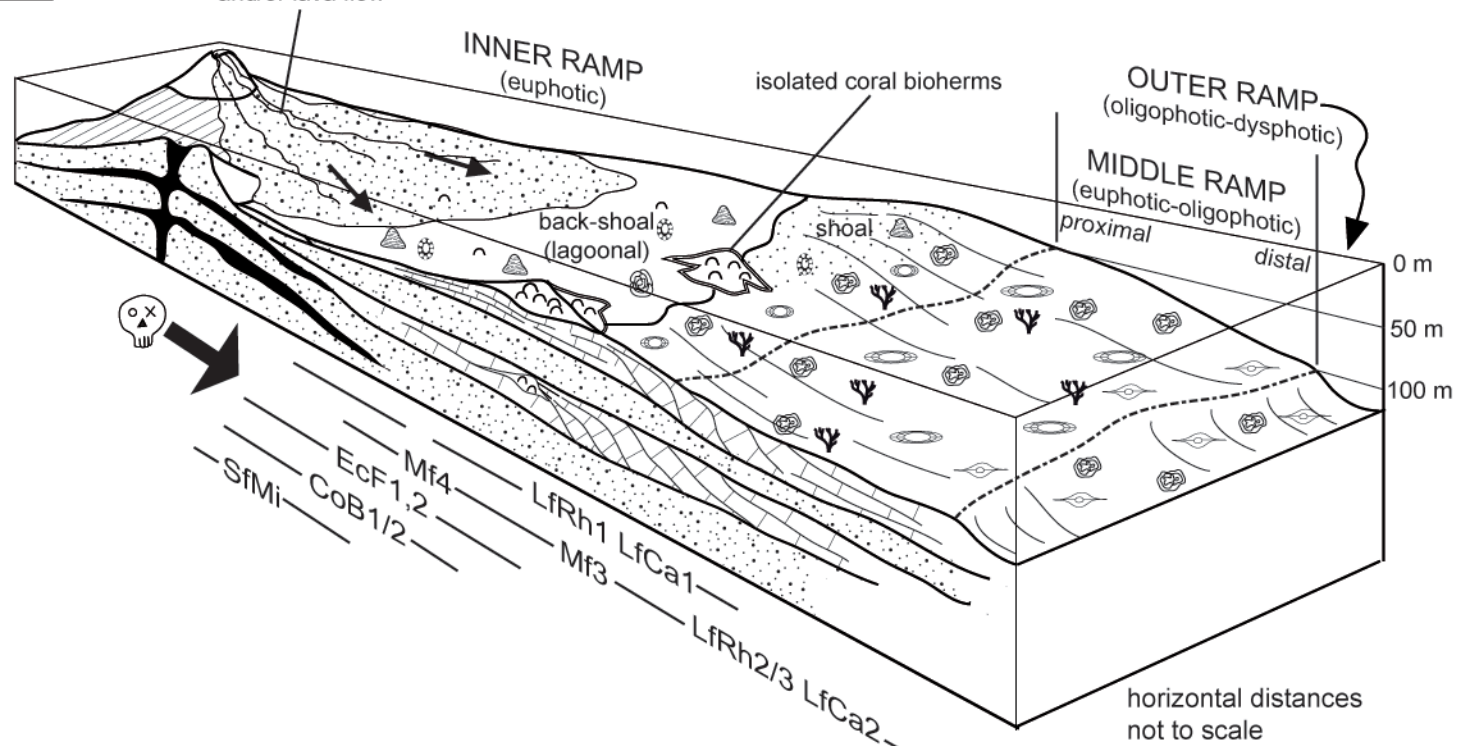
Sedimentary structures

- ⋈ non-specified bioturbation
- ⋈ *Thalassinoides*
- ⋈ volcanic clasts
- ⋈ nodular bedding
- ⊙ concretion

A

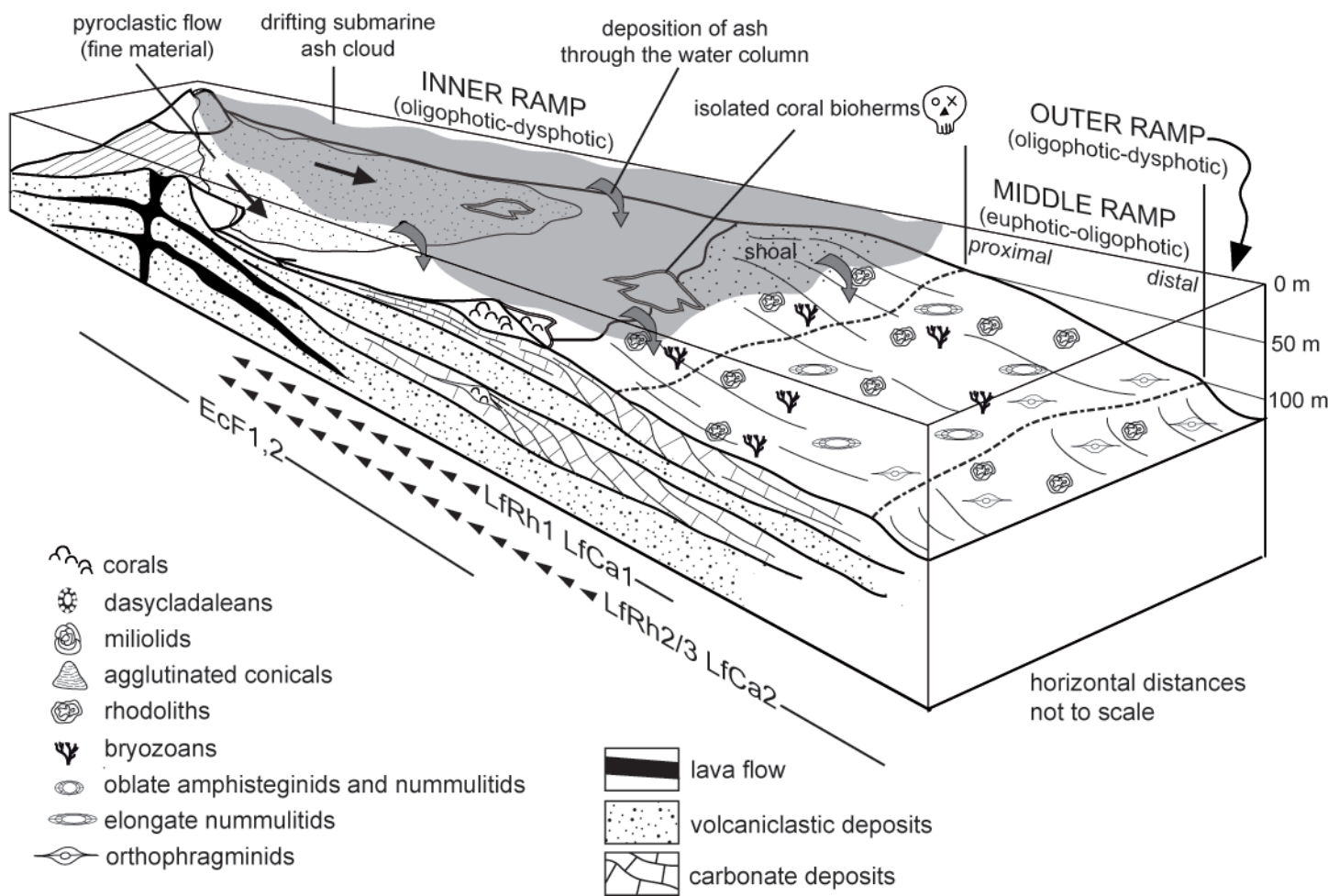
pyroclastic flow (coarse material)
and/or lava flow

Demise of carbonate factories due to pyroclastic flows

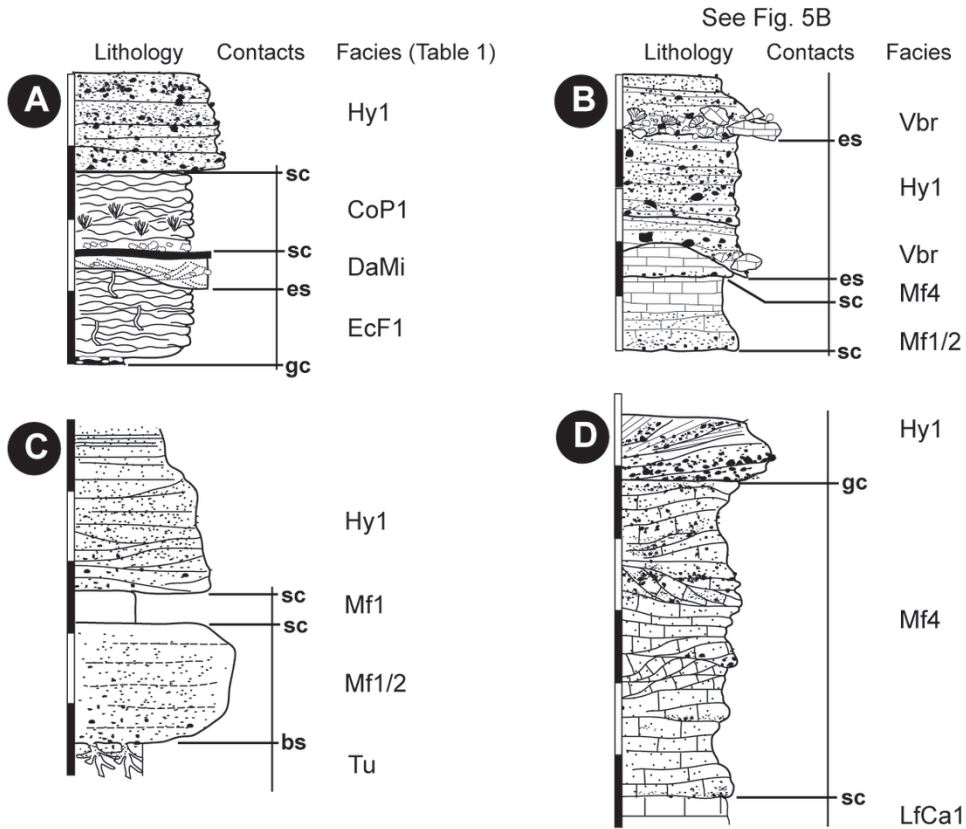


B

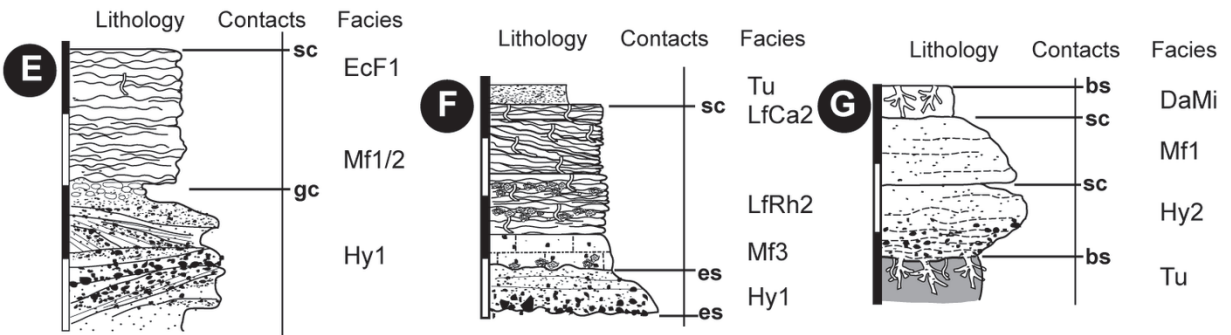
Collapse of carbonate factories caused by deposition of ash



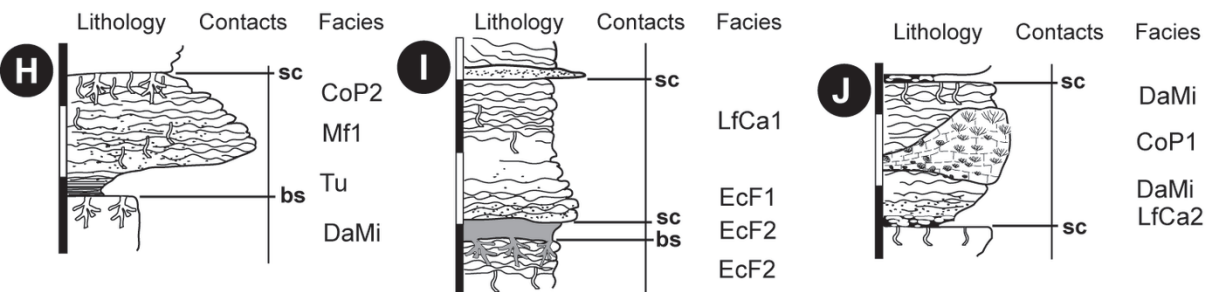
A. Demise of carbonate factories



B. Recovery of carbonate factories

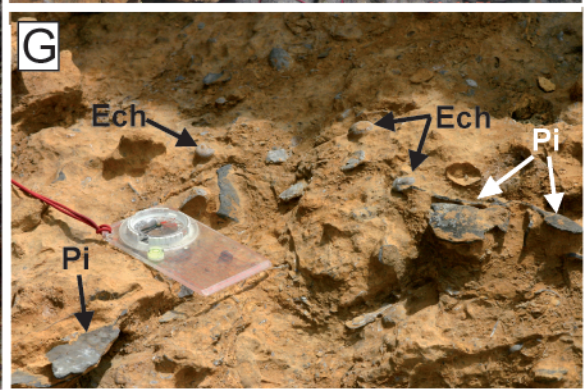
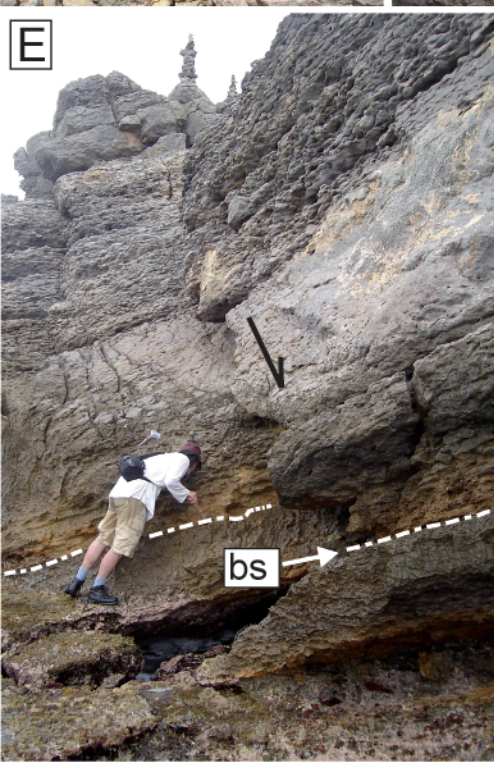
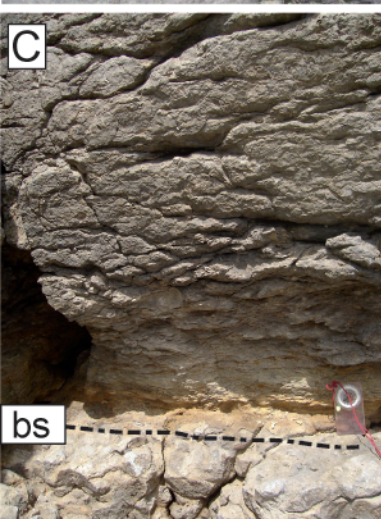
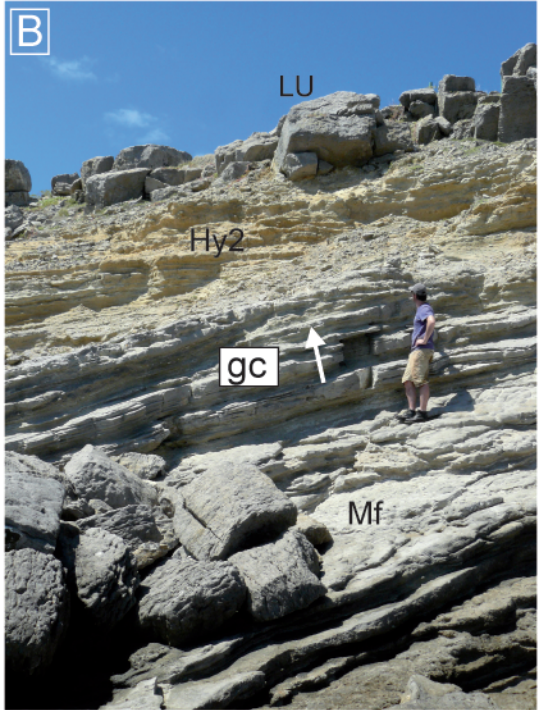
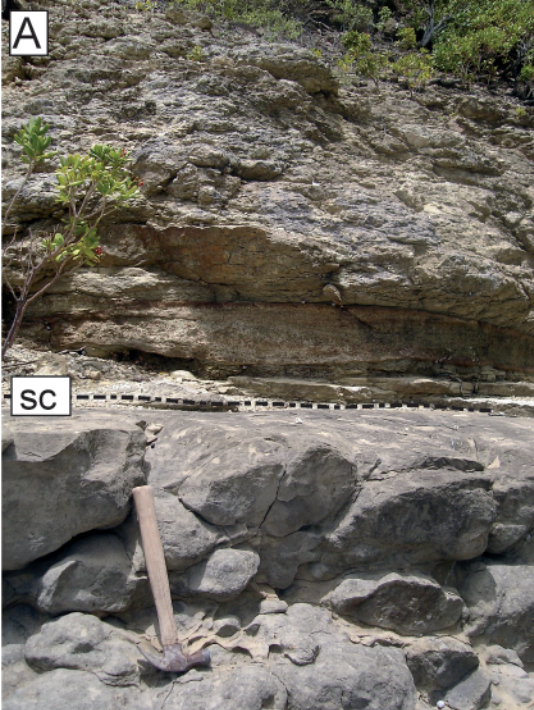


C. Temporarily arrested or slowed carbonate production



Stratigraphic surfaces

es: erosional surface sc: sharp contact
gc: gradational contact bs: burrowed



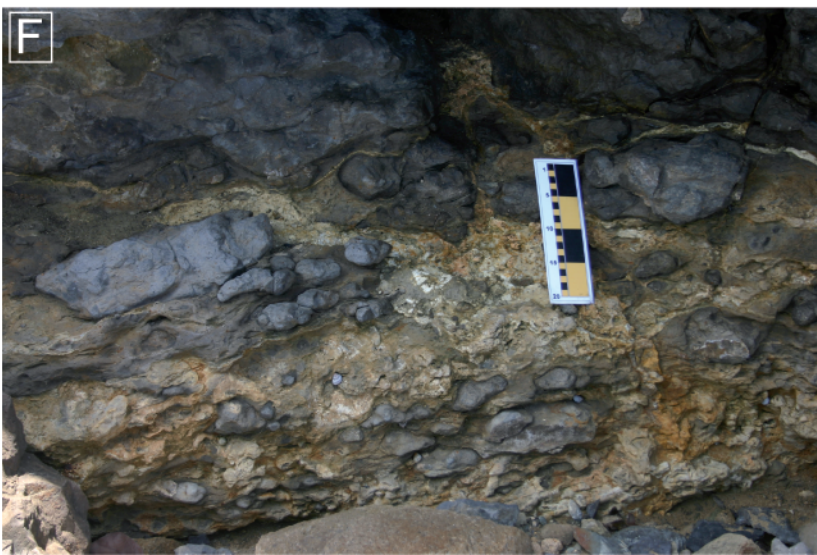
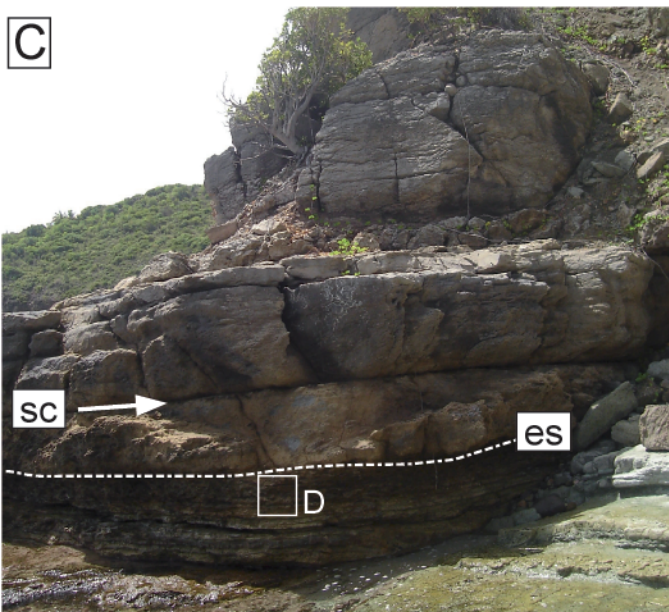
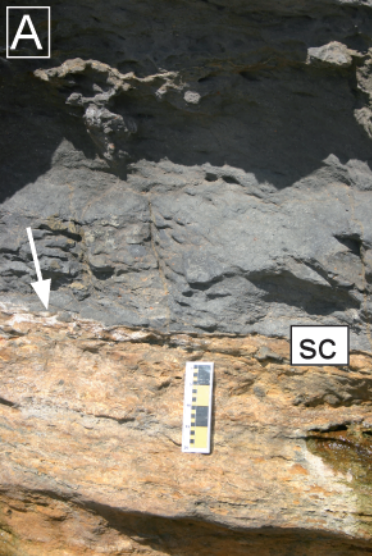


Table 1. Lithofacies in the Eocene limestones of St Bartholemew.

Facies code	Facies after James (1997)	Biotic constituents and skeletal association	Texture	Main skeletal and non skeletal components	Subordinate skeletal and non skeletal components	Taphonomy	Depositional environment
Mixed facies							
MF1	Smaller foraminiferan – dasycladalean – coral photozoan	Foralgal 1 Chloralgal 2 Chlorozoan 3	Ws/Fs, Ps and rarely Gs	Smaller benthic foraminifera. Peloids and micritized grains (cortoids). Agglutinated conical foraminifera and laminar cruts of coralline red algae (<i>Lithoporella</i>).	Miliolids and dasyclad algae. Echinoid (<i>Eupatagus</i> , <i>Antillaster</i>), ostracods, gastropods, bivalves, braching corals and amphisteginids.	Fragmentation : l to m Abrasion : l to m Encrustation : l Bioerosion : m	Inner ramp : shallow back shoal, lagoonal
MF2	Dasycladalean-coral photozoan	Chlorozoan 1 Chloralgal 2 Foralgal 3	Bs Matrix : Fs	Same as MF1 but dominated by branching corals. Gastropods, dasyclad algae and miliolids.	Amphisteginids and nummulitids. Echinoid spatangoids (<i>Antillaster</i>) and agglutinated conical formainifera.	Fragmentation : l to m Abrasion : l tp m Encrustation : m Bioerosion : m	Inner ramp : shallow back shoal, lagoonal
MF3	Echnoid – Red algal photozoan	Echinoforalgal	Ws to Ps/Gs	Echinoids and non-geniculate, small, rhodoliths, coralline branches and laminar cruts Peloids and cortoids.	Large foraminifera (orthophragminids, rare nummulitids and amphisteginids). Bivalves and corals	Fragmentation : m to h Abrasion : m to h Encrustation : l to m Bioerosion : l to m	Distal middle ramp : episodic wave influence
MF4	Larger foraminiferan – molluscan photozoan	Foramol	Ps and/or Gs – volcaniclastic	Larger nummulitids, amphisgenitds and agglunatinated conicals.	Cora land coralline algal, mollusks. Echinoids are found fragedted (<i>Eupatagus</i> , <i>Meoma</i> and <i>Haimea</i>).	Fragmentation : m to h Abrasion : m to h Encrustation : l Bioerosion : l	Open inner ramp to middle ramp : wave-dominated
MF5	Bioclastic – peloidal photozoan	Chloralgal	Ps	Peloids and cortoids.	Benthic formaminifera, echinoid plates and spines, and corals. Thin-shelled mollusks.	Fragmentation : m to h Abrasion : m to h Encrustation : l Bioerosion : h	Inner ramp : shallow back shoal, lagoonal
Carbonate-dominated facies							
DaMi	Dasycladalean algae – miliolid photozoan association	Foralgal 1 Chloralgal 2 Chlorozoan 3	Ws and Ps	Similar to MF1 and MF2. Smaller benthic foraminifera, associated with miliolids and peloids. Dasyclad algae and ostracods. Branching corals and articulated bivalves.	Cortoids, bivalves, agglutinated conicals (<i>Heterodictyoconus</i>) and amphisteginids. Melobesioids.	Fragmentation : l Abrasion : l Encrustation : m to h Bioerosion : m to h	Inner ramp : shallow back shoal, lagoonal
LfRh1	Large bentihc foraminifera – rhodolith photozoan	Rhodalg 1 Foralgal 2	Ps, Rs/Gs and rare Bis	Amphisteginids. Mastophoroids (<i>Litophorella</i>) and sporolithcean (<i>Sporolithon</i>). Melobesioids (<i>Mesophyllum</i> , <i>Lithothamnion</i>). Peloids, oncoids and cortoids. Rhodolthi mean diameter range in size from 1-10 cm. Echinoids (<i>Haimea</i> , <i>Antillaster</i>) and large thick-shelled oysters.	Nummulitids (<i>Nummulites</i>) and lepidocyclinids (<i>Polylepidina</i>). Textulariids, mollusks (epifaunal bivalves), small benthic foraminifers (textulariids, miliolids), encrusting foraminifera (acervulinids), bryozoan, molluks, and corals.	Fragmentation : l to h Abrasion : l to h Encrustation : l to h Bioerosion : l to h	Open inner ramp to middle ramp : wave-dominated
LfRh2	Large bentihc foraminifera – rhodolith photozoan	Rhodalg 1 Foralgal 2	Ps, Rs.	Nummulitids (<i>Nummulites</i>) and lepidocyclinids (<i>Polylepidina</i>). Rhodolthi mean diameter range in size from 1-10 cm.	Amphisteginids, textulariids, mollusks (epifaunal bivalves dominate), coral fragments and planktonic foraminifera. Rare to common peloids and cortoids.	Fragmentation : l to h Abrasion : l to h Encrustation : l to h Bioerosion : l to h	Middle ramp : episodic wave influence
LfRh3	Large bentihc foraminifera – rhodolith photozoan	Rhodalg	Gs	Small rhodoliths. Echinoids and peloids. Rhodolthi mean diameter range in size from 1-5 cm.	Larger benthic foraminifera, mollusks, corals, dasyclad algae and planktonic foraminifera.	Fragmentation : l to h Abrasion : l to h Encrustation : l to h Bioerosion : l to h	Middle ramp : episodic wave influence
LfCa1	Larger benthic foraminiferan – coralline algal photozoan	Foralgal	Ps, Gs	Amphisteginids (<i>Amphistegina</i>). Echinoid, Peloids, cortoids and smaller bentic foraminifera (rotaliids). Subspherical rhodoliths (up to 3 cm diameter). Melobesioids and mastophoroids (<i>Lithoporella</i>).	Nummulitids (<i>Nummulites</i>). Smaller bentic foraminifera (textulariids). Lepidocyclinids (<i>Polylepidinia</i>).	Fragmentation : l to m Abrasion : l to m Encrustation : m Bioerosion : l to m	Open inner ramp to middle ramp : wave-dominated
LfCa2	Larger benthic foraminiferan – coralline algal	Foralgal	Ps, Gs	Nummulitids (<i>Nummulites</i>) and orthophragminids (<i>Discocyclina</i> , <i>Pseudophragmina</i>).	Lepidocyclinids (<i>Polylepidinia</i>).	Fragmentation : l to h Abrasion : l to h Encrustation : l to h	Middle ramp : episodic wave influence

EcF1	photozoan Echnoid – non- skeletal carbonate photozoan	Echinofor Echinoforalgal	Ps, Gs	Echinoid spatangoids (<i>Haimea</i>) and cassiduloids (<i>Echinolampas</i>). Peloids and cortoids.	Corals. Bryozoans. Mollusks. Larger benthic foraminifera (amphisteginids and nummulitids), red algal debris and miliolids.	Bioerosion : l to h Fragmentation : m to h Abrasion : m to h Encrustation : l to m Bioerosion : h	Open inner ramp to middle ramp : wave- dominated
EcF2	photozoan Echnoid – smaleer benthic foraminiferan phtozoan	Echinoforalgal	Ps, Ws	Infaunal and epifaunald echinoids are abundant. Co-occurrence of <i>Haimea</i> , <i>Schizaster</i> , <i>Agassizia</i> , <i>Eupatagus</i> and <i>Echinolampas</i> . Small benthic foraminifera (rotaliids). Mollusks. Peloids.	Large benthic foraminifera. Red algal fragments. Small agglutinated foraminifera, miliolids and calcispheres. Cortoids and oncoids.	Fragmentation : m to h Abrasion : m to h Encrustation : l to m Bioerosion : l to m	Inner ramp : shallow back shoal, lagoonal
CoP1	Coral photozoan	Chlorozoan	Bs Matrix : Ws, Ps, Gs .	Branching and platy corals. Peloids.	Encrusting coralline algae, gastropods, and small benthic foraminifera.	Fragmentation : l to m Abrasion : l to m Encrustation : m Bioerosion : m	Inner ramp : shallow back barrier, lagoonal. Lenticular coral bioherms.
CoP2	Coral photozoan	Chlorozoan	Bs Matrix : Rs	Dendroid corals. Peloids, amphisteginids, nummulitids and orthophragminids, mollusks, coralline red algae.	Dasyclad algae and smaller benthic foraminifera.	Fragmentation : m Abrasion : m Encrustation : m Bioerosion : m to h	Open inner ramp to middle ramp : wave- dominated. Domal coral bioherms